AN EXTENDED ANALYSIS OF THE MULTIPLE MODEL ADAPTIVE CONTROL ALGORITHM

by

Henry Rolan Shomber

B.S., Washington University
(1978)

SUBMITTED IN PARTIAL FULFILLMENT OF THE REQUIREMENTS

FOR THE DEGREE OF

MASTER OF SCIENCE

at the

MASSACHUSETTS INSTITUTE OF TECHNOLOGY

February, 1980

Signature of Author.....
Department of Electrical Engineering
and Computer Science, February 14, 1980

Certified by.....
Thesis Supervisor

Accepted by.....
Chairman, Departmental Committee on Graduate Science

AN EXTENDED ANALYSIS OF THE MULTIPLE
MODEL ADAPTIVE CONTROL ALGORITHM

by

Henry Rolan Shomber

Submitted to the Department of Electrical Engineering and Computer Science on February 14, 1980 in partial fulfillment of the requirements for the degree of Master of Science.

ABSTRACT

One suboptimal control algorithm for systems with unknown dynamics is the Multiple Model Adaptive Control algorithm (MMAC). Due to the potentially wide applicability of this adaptive control algorithm, the properties of this controller need to be understood. This thesis is an extension of previous research into the behavior of deterministic MMAC systems. The investigation undertaken looks at the properties of limited memory, setpoint and stochastic MMAC systems.

The accuracy of approximations developed previously for deterministic hyperbolic MMAC systems is checked, and a modification to improve the accuracy is implemented. A similar approximation is derived for the limited memory and setpoint MMAC systems. The approximations are qualitatively accurate, except in cases where the assumed switch-like behavior in the probabilities did not exist. A modification ensuring the switch-like behavior, using a maximum likelihood control, resulted in an accurate prediction. The need for a stronger stability condition for the setpoint control MMAC is demonstrated.

The analysis of the stochastic MMAC system in this thesis involves two techniques. A Random Input Describing Function (RIDF) approximation is derived for the MMAC system, and Monte Carlo simulations are used to check its accuracy. The accuracy of the RIDF in predicting the first two moments of the states is good for most cases. A modification is suggested which should improve the qualitative and quantitative accuracy of the RIDF. An approximation for the probability density of the MMAC probability indicates that the density accumulates at zero and one for a large class of MMAC systems, i.e., the control uses one model or another, with little use of combinations of the models. The existence of stochastic hyperbolic stability is conjectured along with other stability conjectures based on the observed behavior and approximate analysis.

THESIS SUPERVISOR: Alan S. Willsky

TITLE: Associate Professor, Electrical Engineering and Computer Science

ACKNOWLEDGEMENTS

This completed thesis represents the culmination of work over the last 16 months. It is at this time that I would like to thank those who assisted in its completion. First, I would like to thank Prof. Alan Willsky who as my thesis advisor guided this research, and as my academic counselor provided much advice during my stay at MIT. Secondly, I would like to thank my parents, Henry and Joy Shomber, for their support, both emotionally and financially during this endeavor. I also would like to thank Mrs. Laura Washburn for typing the manuscript and Mr. Arthur Giordani for drafting the figures. Finally, I would like to thank Mr. Larry Vallot for his hospitality over the last month while the thesis was being completed.

This work was supported by the Department of Energy under Contract ET-76-C-01-2295.

TABLE OF CONTENTS

LIST OF FIGURES

LIST OF TABLES

CHAPTER 1

INTRODUCTION

The optimal control problem for systems in which the dynamics are completely known has been thoroughly studied. The theory is well developed, and many techniques are available to determine the optimal control. In the case where the dynamics are incompletely known, the optimal control problem is unsolved. Since the second case is the usual one in control applications, the lack of analytic tools for determining the optimal control has led to the development of numerous suboptimal designs.

In determining the optimal control for the system with known dynamics, the control can usually be determined from calculus of variations [1], Pontryagin's maximum principle [2], or dynamic programming [3]. In the special case of the linear system, linear-quadratic-gaussian methodology can be used to determine the optimal control.

Using dynamic programming to solve for the optimal control for a system with unknown dynamics, Willner [4] proposed a suboptimal controller which is defined in the next section. This algorithm forms the basis for this investigation.

1.1 Definition of the Multiple Model Adaptive Control

Willner [4] attempted to derive an optimal control for a class of systems with unknown dynamics. He limited this class to linear systems

expressible in the following form.

$$\underline{x}(k+1) = \underline{A}(\omega)\underline{x}(k) + \underline{B}(\omega)\underline{u}(k) + \underline{w}(k) \tag{1.1}$$

$$\underline{y}(k+1) = \underline{C}(\omega)\underline{x}(k+1) + \underline{v}(k+1) \tag{1.2}$$

$\underline{x}(k)$ is the plant state vector of dimension n

$\underline{y}(k)$ is the observation vector of dimension m

$\underline{u}(k)$ is the control vector of dimension p

$\underline{w}(k)$, $\underline{v}(k)$ are independent zero mean Gaussian random vectors with covariances $\underline{W}(\omega)$, $\underline{V}(\omega)$ respectively

$\underline{A}(\omega)$, $\underline{B}(\omega)$, $\underline{C}(\omega)$ are the unknown dynamics

ω takes on values in some parameter space Ω, i.e., $\omega \in [0,1]$.

Using the above formulation, along with the following cost function (1.3),

$$J(k) = \varepsilon\left\{\sum_{j=k}^{K} \underline{x}'(j)\underline{Q}(j)\underline{x}(j) + \underline{u}'(j)\underline{R}(j)\underline{u}(j)\right\} \tag{1.3}$$

he attempted to derive the optimal control for the case where ω is constant, and

$$\omega \in \{\omega_i\} \qquad\qquad i = 1,2,\ldots,N$$

i.e., the set of possible dynamics is finite. He showed that the optimal control is extremely complex and could not be implemented practically. A suboptimal control, which was thought to be close to the optimal, was investigated for this case, and was shown to be optimal for the last stage of the dynamic programming solution [4]. This suboptimal control algorithm is the Multiple Model Adaptive Control (MMAC) algorithm, and is defined

as follows.

The plant is assumed linear time invariant and defined by

$$\underline{x}(k+1) = \underline{A}\underline{x}(k) + \underline{B}\underline{u}(k) + \underline{w}(k) \tag{1.4}$$

$$\underline{y}(k+1) = \underline{C}\underline{x}(k+1) + \underline{v}(k+1) \tag{1.5}$$

and the set of models for the possible system dynamics is defined by

$$\underline{x}_i(k+1) = \underline{A}_i\underline{x}_i(k) + \underline{B}_i\underline{u}(k) + \underline{w}_i(k) \tag{1.6}$$

$$\underline{y}_i(k+1) = \underline{C}_i\underline{x}_i(k+1) + \underline{v}_i(k+1) \tag{1.7}$$

where $\underline{w}(k)$, $\underline{v}(k)$, $\underline{w}_i(k)$ and $\underline{v}_i(k)$ are assumed to be stationary. Under these conditions (1.4) - (1.7), the MMAC algorithm is defined by the following equations and is also shown in Figure 1.1.

$$\hat{\underline{x}}_i(k+1) = \underline{A}_i\hat{\underline{x}}_i(k) + \underline{H}_i\underline{r}_i(k+1) \tag{1.8}$$

$$\underline{r}_i(k+1) = \underline{y}(k+1) - \underline{C}_i(\underline{A}_i\hat{\underline{x}}_i(k) + \underline{B}_i\underline{u}(k)) \tag{1.9}$$

$$i = 1,2,\ldots,N$$

$$\underline{H}_i = \underline{S}_i\underline{C}_i'\underline{V}_i^{-1} \tag{1.10}$$

$$\underline{S}_i = [\underline{C}_i'\underline{V}_i\underline{C}_i + (\underline{A}_i\underline{S}_i\underline{A}_i' + \underline{W}_i)^{-1}]^{-1} \tag{1.11}$$

$$\underline{u}(k) = -\sum_{i=1}^{N} P_i\underline{G}_i\hat{\underline{x}}_i(k) \tag{1.12}$$

$$\underline{G}_i = (\underline{B}_i'\underline{K}_i\underline{B}_i + \underline{R}_i)^{-1}\underline{B}_i'\underline{K}_i\underline{A}_i \tag{1.13}$$

$$\underline{K}_i = \underline{Q}_i + \underline{A}_i'\underline{K}_i\underline{A}_i - \underline{A}_i'\underline{K}_i\underline{B}_i(\underline{B}_i'\underline{K}_i\underline{B}_i + \underline{R}_i)^{-1}\underline{B}_i'\underline{K}_i\underline{A}_i \tag{1.14}$$

$$P_i(k+1) = \frac{P_i(k)p(\underline{r}_i(k+1))}{\sum_{j=1}^{N} P_j(k)p(\underline{r}_j(k+1))} \tag{1.15}$$

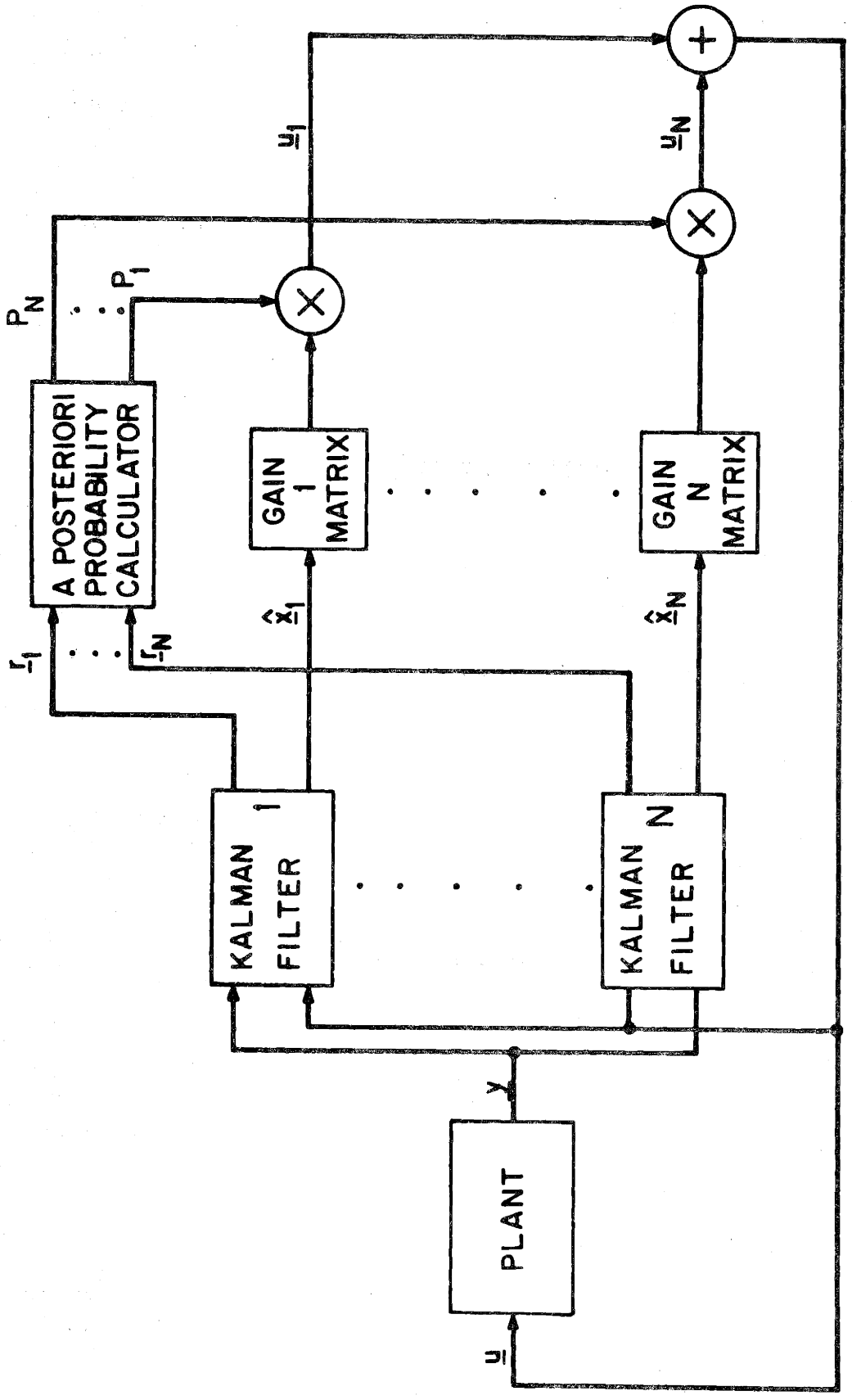

Figure 1.1 Structure of the MMAC System

$$p(\underline{r}_i(k+1)) = ((2\pi)^m \underline{\theta}_i)^{-\frac{1}{2}} \exp(-\tfrac{1}{2}\underline{r}_i'(i+1)\underline{\theta}_i^{-1}\underline{r}_i(k+1)) \tag{1.16}$$

$$\underline{\theta}_i = \underline{V}_i + \underline{C}_i\underline{S}_i\underline{C}_i' \tag{1.17}$$

This set of equations can be divided according to different functions within the MMAC. Estimates of the plant state based on the different models are computed using Eq. (1.8) - (1.11). The equations define steady state Kalman filters based on each model. The driving and observation noise covariances for each model are W_i and V_i, respectively. A feedback gain for the state estimates $\hat{\underline{x}}_i$ based on model i, the state weighting matrix Q_i, and control weighting matrix R_i is computed using Eq. (1.13) - (1.14) (linear quadratic optimal control). Equations (1.15) - (1.18) are used to generate a set of probabilities associated with the models.

1.2 Recent Work

One of the first applications of the MMAC algorithm was the NASA F-8C Digital-Fly-By-Wire Aircraft project [5]. In this application, the F-8C aircraft was used as a testbed for evaluating digital (adaptive) flight controls. In this case, data was available for linearizations of the flight dynamics for various flight conditions in the flight regime. For this application, the models for the MMAC were the linearized flight dynamics.

It should be noted that in this application, the dynamics of the plant were nonlinear and the models were linearizations of the dynamics about various points. This does not fall into the formulation assumed by Willner [4]. The structure of the MMAC algorithm leads to a straight-

forward implementation for this case, but no claim can be made concerning the optimality of this type of application, even for the last stage of the dynamic programming solution.

This application of the MMAC provided a test bed for the performance of the algorithm. For certain sets of models, the algorithm performance was acceptable, while for others its performance was less than satisfactory. The overall performance of the algorithm seemed to be linked to the performance of the identification, i.e., the probabilities.

One of the properties of the MMAC algorithm, demonstrated in the F-8C application, was a switch-like oscillation in the probability. Between switches, the probability was essentially constant, leading to a linear control in the interval. Since the probability had a switch-like oscillation, the resulting control was piecewise linear, with jumps at the probability switch times. It was proposed that the probabilities be low pass filtered to smooth the control. This ad hoc modification did achieve the desired result, without seriously affecting the stabilizing control. This was just one example of the ad hoc procedures used in the implementation of the MMAC for this project.

That further analysis of the MMAC algorithm was necessary became evident with the F-8C application. The effect of the choice of models on the overall performance of the control system was a major question that needed answering. Without this analysis, the control could only be designed and then tested using Monte Carlo techniques, with ad hoc modifications being suggested to improve the performance. The first steps taken toward understanding the properties of the MMAC algorithm were

taken by Greene [6] in his analysis of a simplified MMAC system.

The response exhibited by the MMAC in the F-8C application was thought to have significant deterministic components, and not due entirely to stochastic effects. It was thought that significant portions of the MMAC response could be understood using deterministic analysis. Since the deterministic components needed to be analyzed before work could be done on the stochastic response, Greene's primary assumption was that the white noise sources ($\underline{w}(k)$, $\underline{v}(k)$) were zero. The Kalman filters used in his analysis were designed with assumed nonzero covariances, but for the simulation and the analysis the sources were "turned off." Some significant insights into the behavior of the MMAC system were obtained in this way.

To simplify the analysis, the equations were further reduced with the following additional assumptions:

1. The plant is globally linear
2. The desired closed loop equilibrium state is the origin
3. The matrices $\underline{B}$, $\underline{B}_i$, $\underline{C}$ and $\underline{C}_i$ are identity matrices.

Under the above assumptions, the equations for the two model MMAC analyzed by Greene are:

$$\underline{x}(k+1) = \underline{A}\underline{x}(k) + \underline{u}(k) + \underline{w}(k) \tag{1.18}$$

$$\underline{y}(k+1) = \underline{x}(k+1) + \underline{v}(k+1) \tag{1.19}$$

$$\hat{\underline{x}}_1(k+1) = \underline{A}_1\hat{\underline{x}}_1(k) + \underline{u}(k) + \underline{H}_1\underline{r}_1(k+1) \tag{1.20}$$

$$\underline{r}_1(k+1) = \underline{y}(k+1) - \underline{A}_1\hat{\underline{x}}_1(k) - \underline{u}(k) \tag{1.21}$$

$$\hat{\underline{x}}_2(k+1) = \underline{A}_2\hat{\underline{x}}_2(k) + \underline{u}(k) + \underline{H}_2\underline{r}_2(k+1) \tag{1.22}$$

$$\underline{r}_2(k+1) = \underline{y}(k+1) - \underline{A}_2\hat{\underline{x}}_2(k) - \underline{u}(k) \tag{1.23}$$

$$\underline{u}(k) = -P(k)\underline{G}_1\hat{\underline{x}}_1(k) - (1-P(k))\underline{G}_2\hat{\underline{x}}_2(k) \tag{1.24}$$

$$P(k) = \left(1 - \left(\frac{1-P_0}{P_0}\right)\beta \exp(-\tfrac{1}{2}\alpha(k))\right)^{-1} \tag{1.25}$$

$$\alpha(k+1) = \alpha(k) + \|\underline{r}_1(k+1)\|^2_{\theta_1^{-1}} - \|\underline{r}_2(k+1)\|^2_{\theta_2^{-1}} \tag{1.26}$$

P_0 is the initial probability that model 1 matches the plant

$P(k)$ is the conditional probability that model 1 matches the plant

$$\beta = \sqrt{|\theta_1|/|\theta_2|} \tag{1.27}$$

In this formulation, the probability is a function of the log likelihood ratio $\alpha(k)$. The Kalman filter gains $\underline{H}_1$ and $\underline{H}_2$ are computed using equations (1.10) - (1.11) assuming the following:

$$\underline{W} = \underline{W}_i \tag{1.28}$$

$$\underline{V} = \underline{V}_i \tag{1.29}$$

The control gains $\underline{G}_1$ and $\underline{G}_2$ are computed using equations (1.13) - (1.14), where the following is assumed.

$$\underline{R} = \underline{R}_i \tag{1.30}$$

$$\underline{Q} = \underline{Q}_i \tag{1.31}$$

Using the above formulation Greene was able to demonstrate some of the properties of the MMAC algorithm.

Motivated by the results fo the F-8C application, Greene, as part of his work looked at a "worst case" of the probability switching behavior. Figures 1.2 and 1.3 show a typical "worst case" response for a two state, two model system. This type of response is characterized by large excursions of the states, peaks, and oscillatory switching of the probability. For this case, Greene developed an approximation to the time between switches in the probability and to the size of the states at the switch times.

1.3 Overview of This Thesis

The work in this thesis proceeds in two directions. The first (Chapter 2) is a direct extension of Greene's work, and the second (Chapter 3) is an extension of the analysis to the stochastic MMAC system.

In the direct extension, the accuracy of Greene's approximation to the time between switches is checked for three cases of interest. An equivalent approximation is derived for the single observation finite or limited memory MMAC. The accuracy of this approximation is also checked. The last section is a derivation of a switch time interval approximation for the case of a nonzero set point.

In the extension to the stochastic case a random input describing function (RIDF) is computed for the two model MMAC system. This approximation is compared to Monte Carlo simulation results for various cases.

1.4 Notation

Listed in this section are some definitions used later in this thesis.

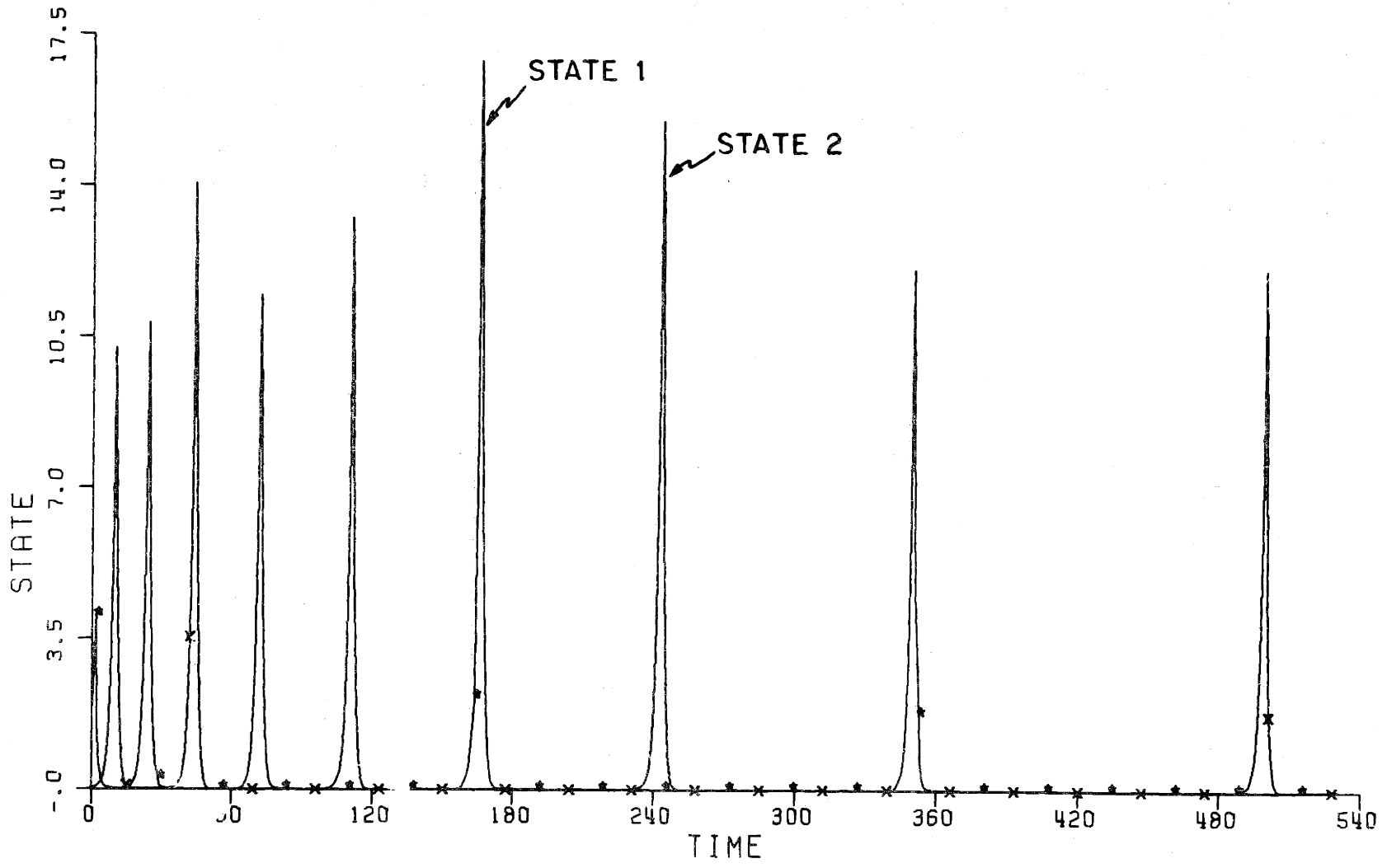

Figure 1.2 Typical "Worst Case" MMAC Response (Plant States)

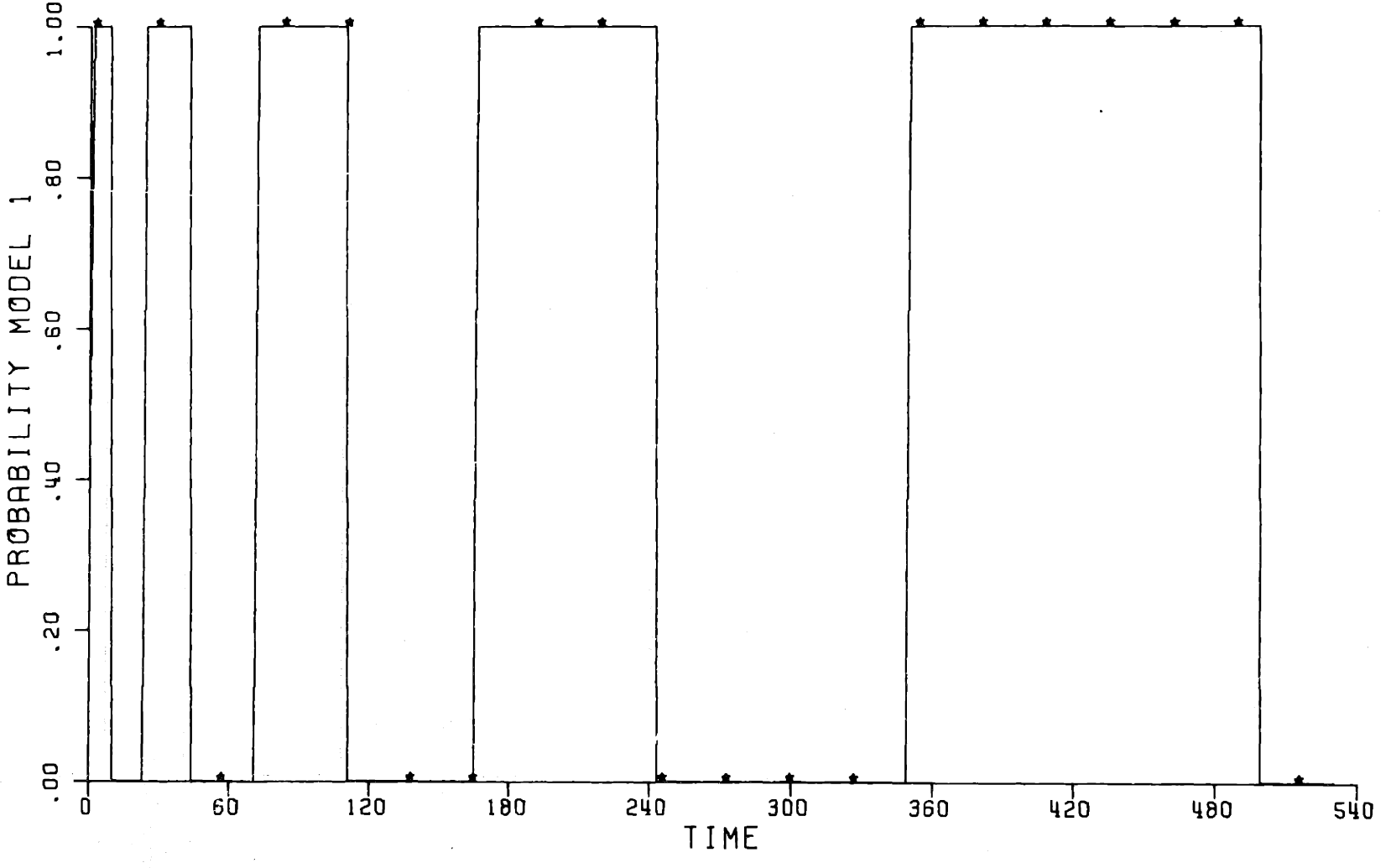

Figure 1.3 Typical "Worst Case" MMAC Response (Probability)

$\|\underline{A}\|^2 = \max\lambda(\underline{A}'\underline{A})$

$\|\underline{A}\|_*^2 = \max(\lambda(\underline{A}))^2$ (note this is not a true norm)

$\lambda(\underline{A})$ = eigenvalues of $\underline{A}$

$\|\underline{x}\| = \sqrt{\underline{x}'\underline{x}}$

$\|\underline{x}\|_{\underline{\theta}} = \sqrt{\underline{x}'\underline{\theta}\underline{x}}$

$|\underline{A}|$ = determinant of $\underline{A}$

CHAPTER 2

DETERMINISTIC ANALYSIS

In this chapter, some of Greene's analysis of a "worst case" MMAC system are reviewed, checked for accuracy, and then extended to two other formulations of the algorithm. Using this type of analysis, qualitative results concerning the response of the MMAC can be obtained.

Section 2.1 is essentially a review of Greene's derivation of the approximation for the time between switches in the probability. This is included as a reference for the type of approximation derived in Sections 2.2 and 2.3. Also, in checking Greene's approximation it became necessary to implement a modification to the approximation, and inclusion of Greene's derivation gives some insight into the effects of this modification.

Section 2.2 is a derivation of an approximation to the time between switches for the single observation limited memory MMAC algorithm. In this algorithm, the MMAC probabilities are based only on the last observation, $\underline{y}(k)$, and not on all past observations. This algorithm is an example of what Greene referred to as the Finite Memory MMAC [6]. The accuracy of this approximation is checked using simulations of the system for three different cases.

Section 2.3 is a derivation of an approximation of the time between switches in the probability for a nonzero set point MMAC. For this case, the desired equilibrium is no longer the origin, as the possibility of biases in the control inputs is allowed.

In this chapter, the cases used for the comparison of the accuracy of the approximations are defined in Table 2.1. These three cases correspond to stable, neutrally stable, and unstable MMAC systems. The stability of the system can be seen in the change in the height of the peaks of the state in the responses, Figures 2.1, 2.2, and 2.3. The system is stable if the height of the peaks decreases with time, neutrally stable if the height of the peaks is constant with time, and unstable if the height of the peaks increases with time. Further insight into these types of stability can be obtained in Section 2.1.

2.1 A Review of Greene's Switch Time Approximation Derivation

An alternate expression for the MMAC was used in Greene's analysis. In this alternate form, the state of the MMAC system was taken to be the plant state augmented by the filter residuals, instead of the filter estimates, and the probability;

$$\begin{bmatrix} \underline{x}(k+1) \\ \underline{r}_1(k+1) \\ \underline{r}_2(k+1) \end{bmatrix} = \tilde{\underline{A}}(P(k)) \begin{bmatrix} \underline{x}(k) \\ \underline{r}_1(k) \\ \underline{r}_2(k) \end{bmatrix} \tag{2.1}$$

$$\tilde{\underline{A}}(P(k)) = \begin{bmatrix} \underline{A} - P(k)\underline{G}_1 - (1-P(k))\underline{G}_2 & P(k)\underline{G}_1(\underline{I} - \underline{H}_1) & (1-P(k))\underline{G}_2(\underline{I} - \underline{H}_2) \\ \underline{A} - \underline{A}_1 & \underline{A}_1(\underline{I} - \underline{H}_1) & 0 \\ \underline{A} - \underline{A}_2 & 0 & \underline{A}_2(\underline{I} - \underline{H}_2) \end{bmatrix} \tag{2.2}$$

Using equations (2.1) - (2.2) along with equations (1.25) - (1.27), instead of equations (1.18) - (1.27), simplified the analysis.

TABLE 2.1: Deterministic Case Definition

$$\underline{A} = \begin{bmatrix} a & 0 \\ 0 & a \end{bmatrix} \qquad \underline{A}_1 = \begin{bmatrix} a_1 & 0 \\ 0 & a \end{bmatrix} \qquad \underline{A}_2 = \begin{bmatrix} a & 0 \\ 0 & a_1 \end{bmatrix}$$

$$\underline{H}_1 = \begin{bmatrix} h & 0 \\ 0 & h_1 \end{bmatrix} \qquad \underline{H}_2 = \begin{bmatrix} h_1 & 0 \\ 0 & h \end{bmatrix}$$

$$\underline{G}_1 = \begin{bmatrix} g & 0 \\ 0 & g_1 \end{bmatrix} \qquad \underline{G}_2 = \begin{bmatrix} g_1 & 0 \\ 0 & g \end{bmatrix}$$

Case	$\underline{a}$	$\underline{a}_1$	$\underline{h}$	$\underline{h}_1$	$\underline{g}$	$\underline{g}_1$
a	2.0	0.	0.809	0.5	1.62	0.
b	2.0	0.	0.809	0.5	1.50	0.
c	2.0	0.	0.809	0.5	1.40	0.

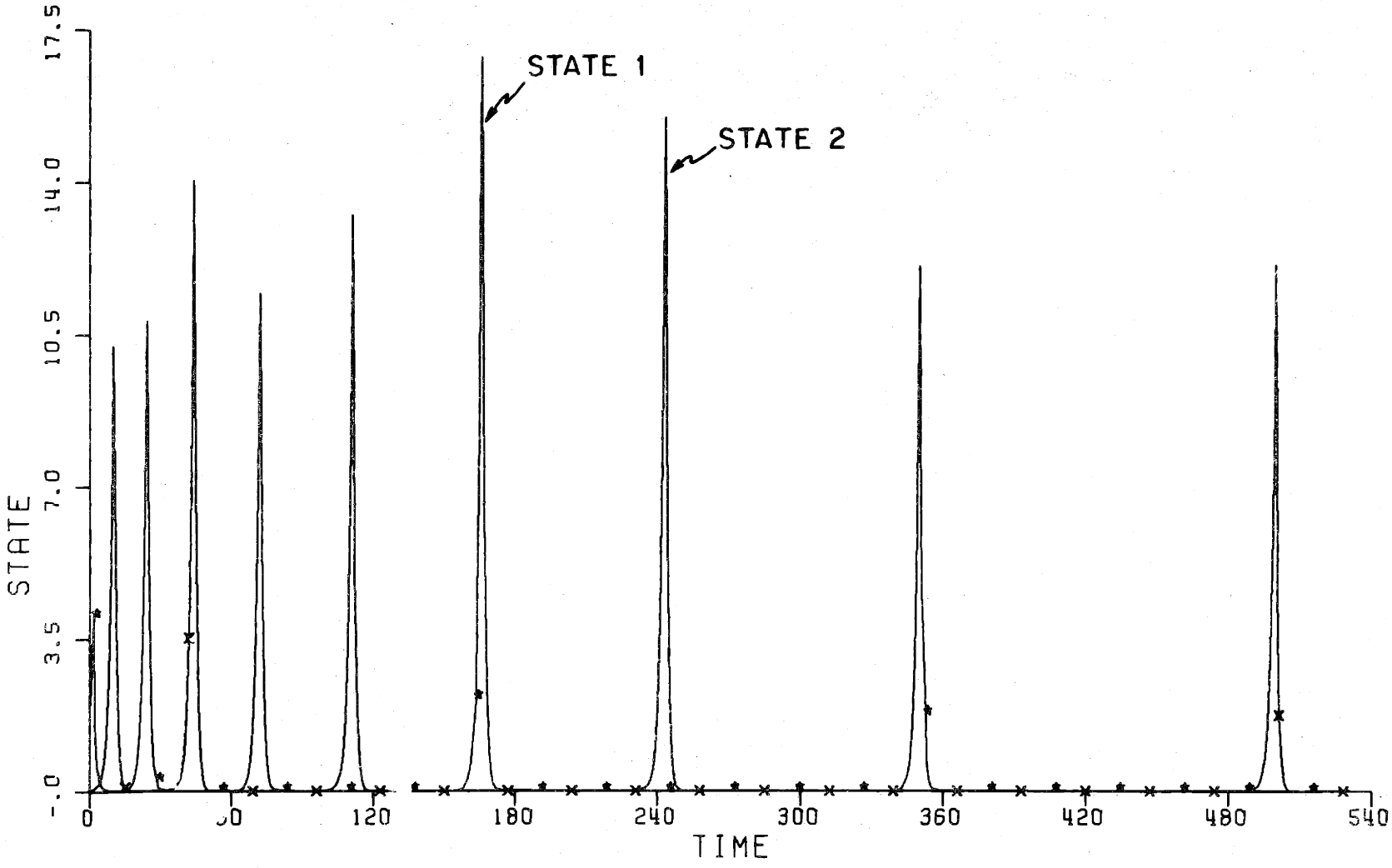

Figure 2.1 Stable Hyperbolic Oscillations

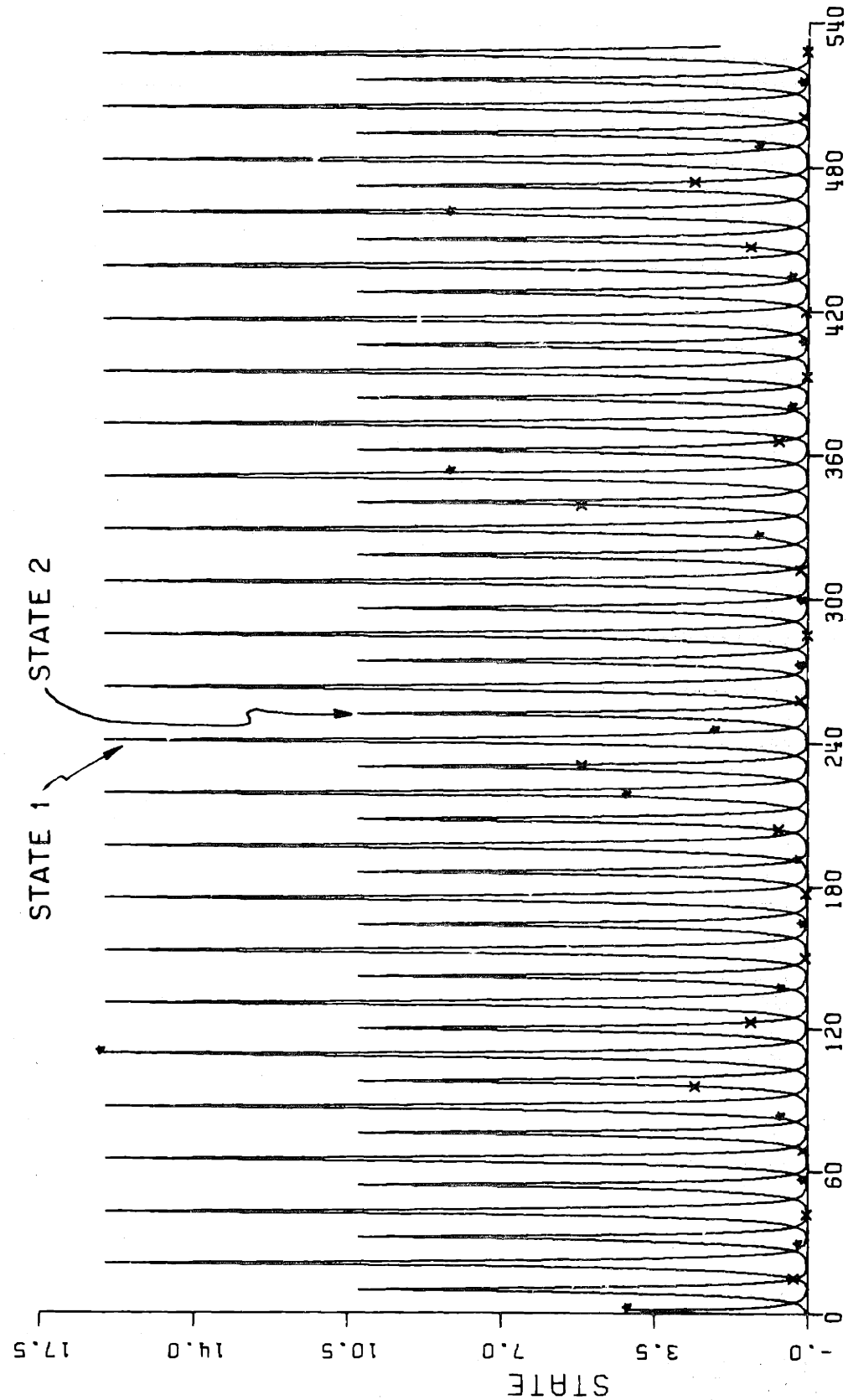

Figure 2.2 Neutrally Stable Hyperbolic Oscillations

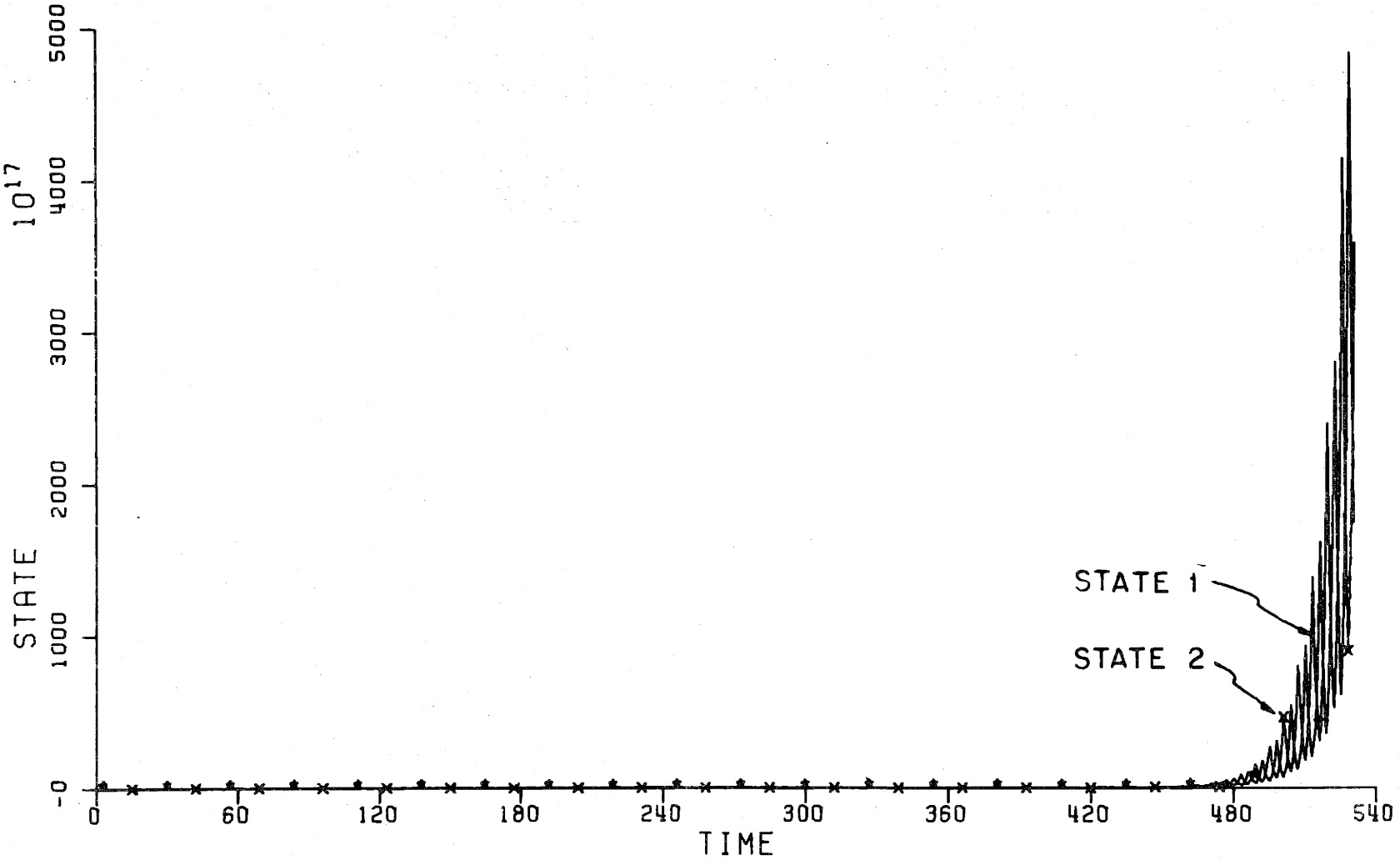

Figure 2.3 Unstable Hyperbolic Oscillations

One of the advantages of this formulation is that the system is linear for a fixed value of the probability (P(k)). This allows the use of some of the insights of linear system theory in the analysis of the properties of the system. For example, if $\tilde{\underline{A}}(P(k))$ is stable, i.e.,

$$\max|\lambda(\underline{A}(P))| < 1 \qquad \forall\ P \in [0,1]$$

then the system is stable, [6]. Greene called this type of stability universal stability.

For the case of interest in this chapter, $\tilde{\underline{A}}(P(k))$ is unstable for all P(k).

$$\max|\lambda(\underline{A}(P))| > 1 \qquad \forall\ P \in [0,1]$$

Greene found certain conditions on $\tilde{\underline{A}}(P(k))$ such that it was unstable for all P(k), but the MMAC system was still stable. The primary assumption for this type of stability was that each mode of the system is stabilized for P(k) equalling either 1 or 0 (although some modes may not be stabilized for both 0 and 1).

With this assumption in mind, a new set of state vectors, $\underline{y}_1(i)$ and $\underline{y}_2(k)$ were defined. The states $\underline{y}_1(k)$ were unstable for P(k) = 0 and the states $\underline{y}_2(k)$ were unstable for P(k) = 1. The matrices A, A_1 and A_2 were assumed to be diagonal, which allowed the following partition of $\underline{A}(P(k))$.

$$\begin{bmatrix} \underline{y}_1(k+1) \\ \underline{y}_2(k+1) \end{bmatrix} = \begin{bmatrix} \tilde{\underline{A}}_1(P(k)) & 0 \\ 0 & \tilde{\underline{A}}_2(P(k)) \end{bmatrix} \begin{bmatrix} \underline{y}_1(k) \\ \underline{y}_2(k) \end{bmatrix} \tag{2.3}$$

where

$$\begin{bmatrix} \tilde{\underline{A}}_1(P(k)) & 0 \\ 0 & \tilde{\underline{A}}_2(P(k)) \end{bmatrix}$$

is an appropriately partitioned version of $\tilde{\underline{A}}(P(k))$.

Simulations demonstrated a switch-like behavior in the probability for this MMAC system. The probability P(k) would switch from near zero to near one and vice versa as the plant states were alternately stabilized and destabilized.

To characterize this type of behavior, Greene introduced the concept of hyperbolic oscillations, with a corresponding stability concept. If the unstable states for $P(k) = 1$ (or 0) increase at a slower rate during the time interval where $P(k) = 0$ (or 1), then the system was called <u>hyperbolically stable</u>. If the rate of decay is equal to the rate of growth, then the system response was neutrally stable hyperbolic oscillations, otherwise the system was hyperbolically unstable.

Motivated by the simulations, Greene assumed the probability is 1 or 0 in the interval between switches in the probability. In actuality, the probability is not 0 or 1, but the assumption that it takes on these values is not unreasonable, since on these intervals, the values of the probability are nearly zero or one. Greene developed an approximation to the time between switches in the probability and to the norm of the state vectors $\underline{y}_1(k)$ and $\underline{y}_2(k)$ at the switch times, $\{T_j\}$. We now review this development. Let

$$P(k) = \begin{cases} 0 & T_{j-1} \leq k < T_j \\ 1 & T_j \leq k < T_{j+1} \end{cases} \qquad (2.4)$$

$$\|\underline{y}_1(T_{j-1})\|^2 < \|\underline{y}_2(T_{j-1})\|^2 \tag{2.5}$$

During the interval $[T_{j-1}, T_j)$, $\|\underline{y}_1(k)\|^2$ increases and $\|\underline{y}_2(k)\|^2$ decreases. At the switch time, T_j,

$$\|\underline{y}_1(T_j)\|^2 > \|\underline{y}_2(T_j)\|^2 \tag{2.6}$$

and during the next interval $[T_j, T_{j+1})$, $\|\underline{y}_1(k)\|^2$ decreases, and $\|\underline{y}_2(k)\|^2$ increases.

The relation between the above approximation and the concepts of hyperbolic stability is as follows: for j sufficiently large,

Stable Hyperbolic Oscillations

$$\|\underline{y}_1(T_j)\|^2 > \|\underline{y}_1(T_{j+2})\|^2 \quad \text{and} \quad \|\underline{y}_2(T_{j-1})\|^2 > \|\underline{y}_2(T_j)\|^2 \tag{2.7}$$

Neutrally Stable Hyperbolic Oscillations

$$\|\underline{y}_1(T_j)\|^2 = \|\underline{y}_1(T_{j+2})\|^2 \quad \text{and} \quad \|\underline{y}_2(T_{j-1})\|^2 = \|\underline{y}_2(T_j)\|^2 \tag{2.8}$$

Unstable Hyperbolic Oscillations

$$\|\underline{y}_1(T_j)\|^2 < \|\underline{y}_1(T_{j+2})\|^2 \quad \text{and} \quad \|\underline{y}_2(T_{j-1})\|^2 < \|\underline{y}_2(T_j)\|^2 \tag{2.9}$$

Using the equations (2.3), (1.25) - (1.27) for the evolution of $\underline{y}_1(k)$, $\underline{y}_2(k)$ and $\alpha(k)$, the time interval between switches in the probability can be approximated. In the two model, two dimensional state case used in Greene's examples $\underline{y}_1(k)$ and $\underline{y}_2(k)$ are defined as follows.

$$\underline{y}_1(k) = \begin{bmatrix} x_1(k) \\ r_{11}(k) \\ r_{12}(k) \end{bmatrix} \qquad \underline{y}_2(k) = \begin{bmatrix} x_2(k) \\ r_{21}(k) \\ r_{22}(k) \end{bmatrix} \tag{2.10}$$

where

$$\text{Plant state} \qquad \underline{x}(k) = \begin{bmatrix} x_1(k) \\ x_2(k) \end{bmatrix} \tag{2.11}$$

$$\text{Filter 1 residual} \qquad \underline{r}_1(k) = \begin{bmatrix} r_{11}(k) \\ r_{12}(k) \end{bmatrix} \tag{2.12}$$

$$\text{Filter 2 residual} \qquad \underline{r}_2(k) = \begin{bmatrix} r_{21}(k) \\ r_{22}(k) \end{bmatrix} \tag{2.13}$$

so the evolution of $\alpha(k)$ can be written as follows:

$$\begin{aligned} \alpha(k) = \sum_{i=0}^{k} & \underline{y}_1'(i) \prod_{\ell=0}^{i} \tilde{\underline{A}}_1'(P(\ell)) \, \underline{\Phi}_1 \prod_{\ell=0}^{i} \tilde{\underline{A}}_1(P(\ell)) \, \underline{y}_1(i) \\ & - \underline{y}_2'(i) \prod_{\ell=0}^{i} \tilde{\underline{A}}_2'(P(\ell)) \, \underline{\Phi}_2 \prod_{\ell=0}^{i} \tilde{\underline{A}}_2(P(\ell)) \, \underline{y}_2(i) \end{aligned} \tag{2.14}$$

where Φ_1 and Φ_2 are appropriately partitioned versions of $\underline{\theta}_1^{-1}$ and $\underline{\theta}_2^{-1}$.

For

$$K \in [T_j, T_{j+1})$$

then

$$P(k) \simeq 0 \tag{2.15}$$

then assuming

$$P(k) = 0 \tag{2.16}$$

leads to

$$\tilde{\underline{A}}_1(P(k)) = \tilde{\underline{A}}_1(0) \tag{2.17}$$

$$\tilde{\underline{A}}_2(P(k)) = \tilde{\underline{A}}_2(0) \tag{2.18}$$

if

$$a_1 = \|\tilde{\underline{A}}_1(0)\|^2 \tag{2.19}$$

$$a_2 = \|\tilde{\underline{A}}_2(0)\|^2 \tag{2.20}$$

then on this interval

$$a_1 > 1 \tag{2.21}$$

$$a_2 < 1 \tag{2.22}$$

and

$$\alpha(k) \simeq \alpha(T_j) + \sum_{x=T_j}^{T_{j+1}-1} a_1^{k-T_j} \|\underline{y}_1(T_j)\|^2\sigma_1 - a_2^{k-T_j} \|\underline{y}_2(T_j)\|^2\sigma_2 \tag{2.23}$$

where

$$\sigma_1 = \|\underline{\phi}_1\| \tag{2.24}$$

$$\sigma_2 = \|\underline{\phi}_2\| \tag{2.25}$$

At the switch times,

$$\alpha(T_j) \simeq 0 \tag{2.26}$$

$$\alpha(T_{j+1}) \simeq 0 \tag{2.27}$$

$$\|\underline{y}_1(T_j)\|^2 < \|\underline{y}_2(T_j)\|^2 \tag{2.28}$$

If the half period for the oscillation, T, is defined as follows:

$$T = T_{j+1} - T_j \tag{2.29}$$

then T can be approximated from the following equation.

$$\frac{a_1^{T+1} - 1}{a_1 - 1} \|\underline{y}_1(T_j)\|^2 \sigma_1 = \frac{a_2^{T+1} - 1}{a_2 - 1} \|\underline{y}_2(T_j)\|^2 \sigma_2 \tag{2.30}$$

As Greene noted, exact solution of this equation (2.30) for T, is not possible, but T can be approximated using numerical techniques.

This approximation will be checked using the three cases defined in Table 2.1. These cases correspond to the three types of hyperbolic stability, for which the approximation was derived. The stability of each case is defined below.

Case a) Stable Hyperbolic Oscillations

b) Neutrally Stable Hyperbolic Oscillations

c) Unstable Hyperbolic Oscillations

2.2 Implementation of Greene's Switch Time Approximation

The approximation to the switch times and the norms of the states derived by Greene, outlined in the previous section (2.1), appears to be

quite useful. Greene showed this approximation should allow insights to be gained concerning the type of response of the MMAC system. The actual implementation of the approximation was not done, i.e., no specific cases were checked.

The work done in this section is a check of the accuracy of Greene's approximation, something not done in his thesis. Similar approximations are derived for two other MMAC formulations later in this chapter, so a check on the accuracy of this type of approximation, switch time, seems prudent.

Difficulties were encountered in the computation of the norms of the matrices in Greene's approximation. In the derivation of the approximation it was assumed that:

$$\|\tilde{\underline{A}}_1(0)\|^2 > 1 \tag{2.31}$$

$$\|\tilde{\underline{A}}_2(0)\|^2 < 1 \tag{2.32}$$

but the values computed for these norms were not as expected. Instead of $\|\tilde{\underline{A}}_i(P)\|^2$ being greater than one for $P = 1$ (or 0) and less than one for $P = 0$ (or 1), it was strictly greater than one, Table 2.2.

Using the values for the norms, it is obvious that the approximation will indicate instability independent of the stability of the actual MMAC system. Since the norms are greater than one for $P = 1$ and $P = 0$, the estimates of $\|\underline{y}_2(k)\|^2$ and $\|\underline{y}_2(k)\|^2$ generated by the approximation will grow with time, ruling out any behavior similar to stable hyperbolic oscillations.

TABLE 2.2: $||\tilde{\underline{A}}_i(P)||^2$ for Deterministic Cases

CASE	P	$\|\|\tilde{\underline{A}}_1(P)\|\|^2$	$\|\|\tilde{\underline{A}}_2(P)\|\|^2$
a	0.	8.00	4.15
	1.	4.15	8.00
b	0.	8.00	4.23
	1.	4.23	8.00
c	0.	8.00	4.37
	1.	4.37	8.00

Greene had suggested using the following measure of the size of the matrix (quasi-norm):

$$||\underline{A}||^2 = \max(\lambda(\underline{A}))^2 \tag{2.33}$$

instead of the norm

$$||\underline{A}||^2 = \max\lambda(\underline{A}'\underline{A}) \tag{2.34}$$

It was suggested in [6] that this might result in an improvement in the approximation. Thus the use of this quantity was investigated.

It is easily shown that $||(\cdot)||_*$ is not a true norm. However, it in fact does improve the approximation, as is seen later. Also as is seen in Table 2.3, the values assumed for the matrices have the expected properties, i.e., the matrices $\tilde{\underline{A}}_i(P)$ were not stable for $P = 0$ or $P = 1$.

To determine the accuracy of the approximation, in predicting the switch times and the corresponding magnitude of the states, a measure of the size of the states is needed. Greene developed a quasi-Lyapunov function to measure the growth or decay of the states of the plant

$$V(k) = \ln \underline{x}_1(k)\underline{x}_2(k) \tag{2.35}$$

Although (2.35) is not a true Lyapunov function, it gives a good indication of the stability of the system in the hyperbolic sense. Since the plant states are not computed in the approximation of the switch times, a modified function was chosen for this analysis of the accuracy of Greene's approximation. This second quasi-Lyapunov function uses parameters which are computed in the approximation

TABLE 2.3: $\|\tilde{\underline{A}}_i(P)\|_*^2$ for Deterministic Cases

CASE	P	$\|\tilde{\underline{A}}_1(P)\|_*^2$	$\|\tilde{\underline{A}}_2(P)\|_*^2$
a	0.	4.00	0.14
	1.	0.14	4.00
b	0.	4.00	0.25
	1.	0.25	4.00
c	0.	4.00	0.36
	1.	0.36	4.00

$$V^*(k) = \ln\|\underline{y}_1(k)\|^2\|\underline{y}_2(k)\|^2 \tag{2.36}$$

This function is quite similar to Greene's quasi-Lyapunov function, and consequently has similar properties with regard to the stability of the system.

For the cases of interest, the function V* behaves linearly with time as does Greene's [6]. The increment of the linear function V* is indicative of the stability of the system.

$V^*(k+1) - V^*(k) < 0$	Stable Hyperbolic Oscillations
$V^*(k+1) - V^*(k) = 0$	Neutrally Stable Hyperbolic Oscillations
$V^*(k+1) - V^*(k) > 0$	Unstable Hyperbolic Oscillations

This linearity with time, exploited by Greene in his analysis, is also quite useful in this work, so V* will be repeatedly used in this approximate stability analysis.

To obtain a comparison of the approximation to the actual system response, V* is plotted at the switch times (Figures 2.4a, 2.4b, 2.4c). In these figures, V* from the simulation results is plotted at the actual probability switch time. For the sake of contrast, V*, as predicted by the approximation, is plotted at the predicted switch times, also from the approximation. By plotting the data in this way the accuracy of the approximation for both the size of the states and switch times is seen.

It is apparent from the figures that the approximation is not an exact prediction of the behavior of the system, but that it is indicative of the response. The error in predicting the times of probability transitions (T_j) is significant as is the error in predicting the size of the

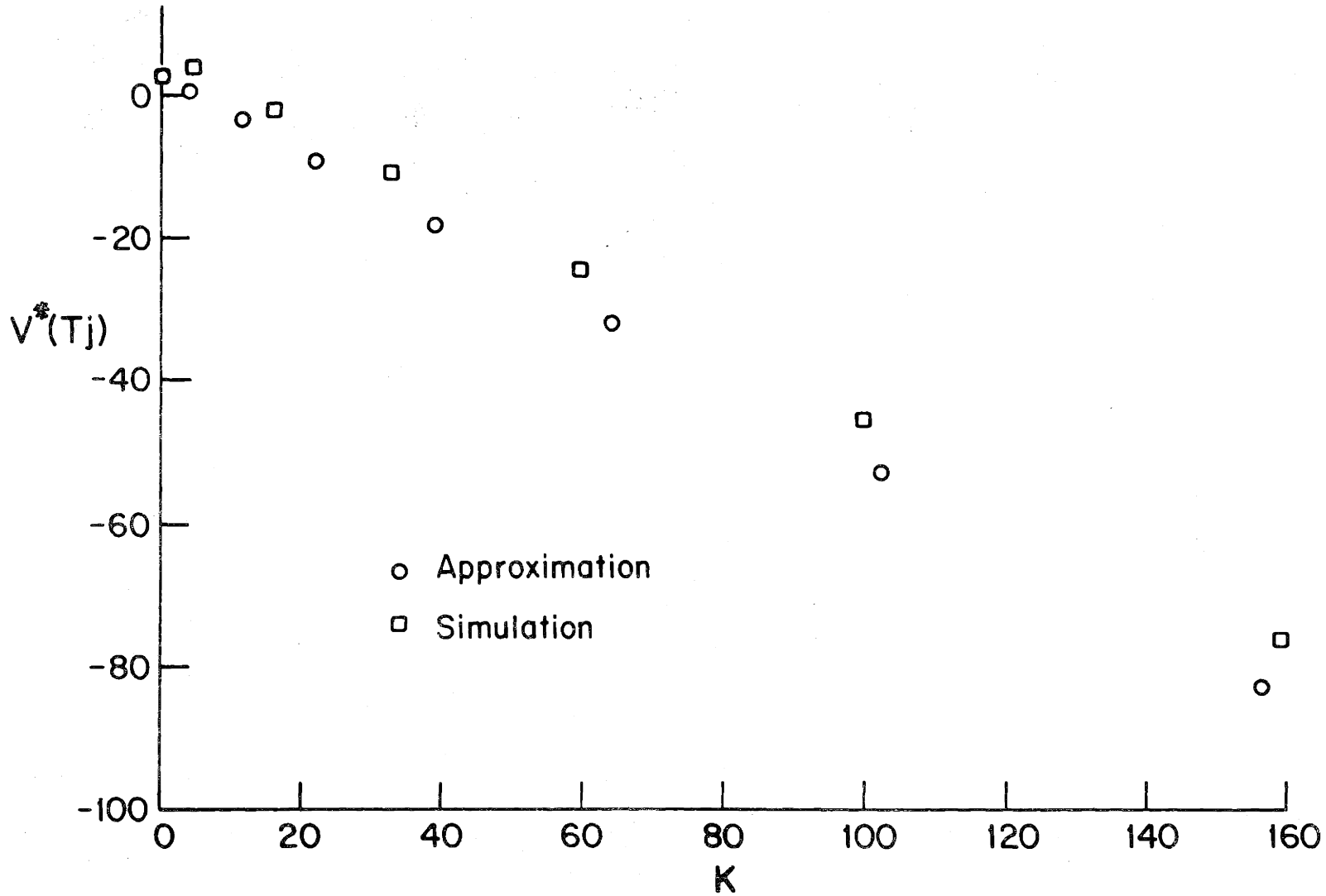

Figure 2.4a $V^*(T_j)$ for Simulation and Approximation

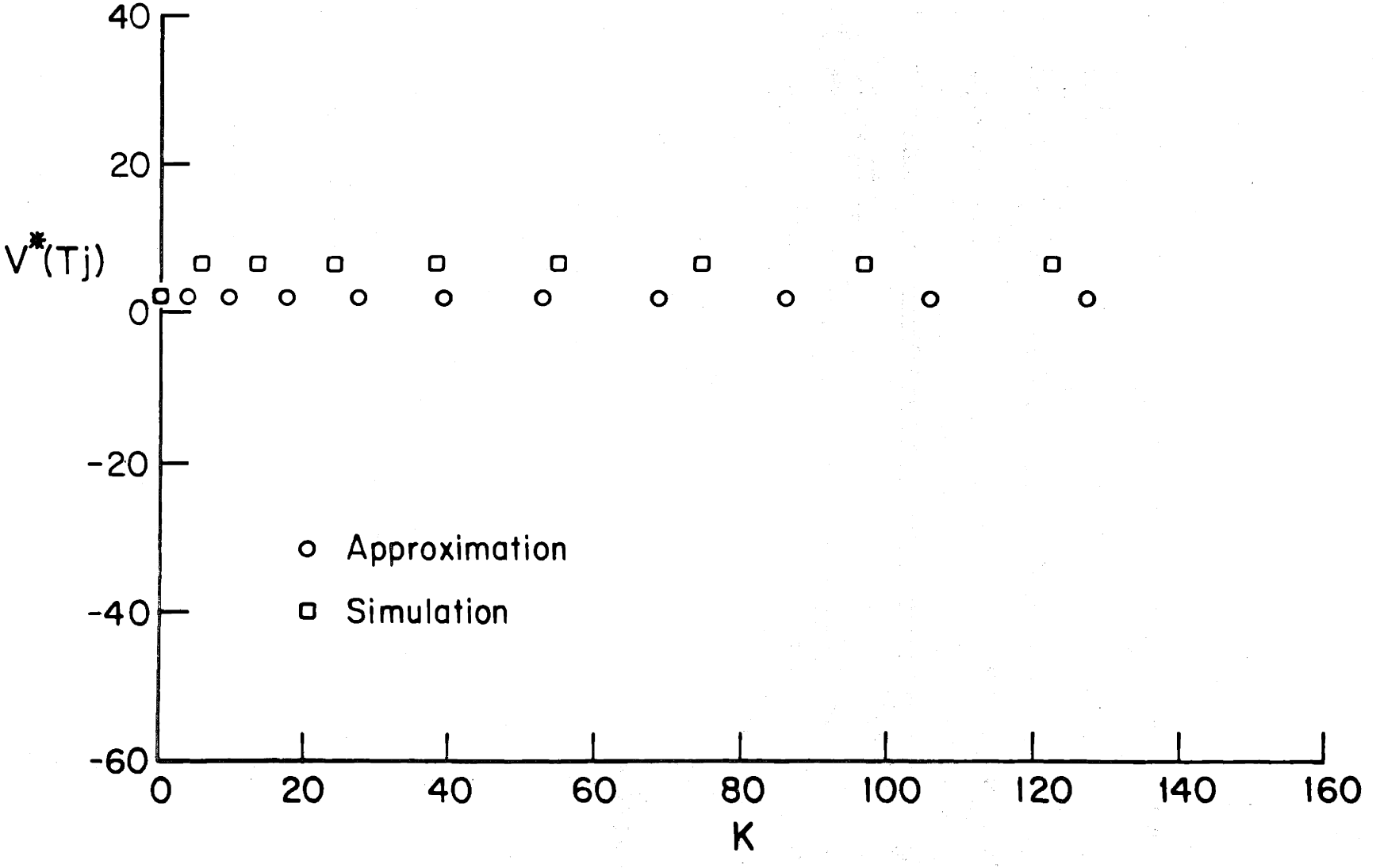

Figure 2.4b $V^*(T_j)$ for Simulation and Approximation

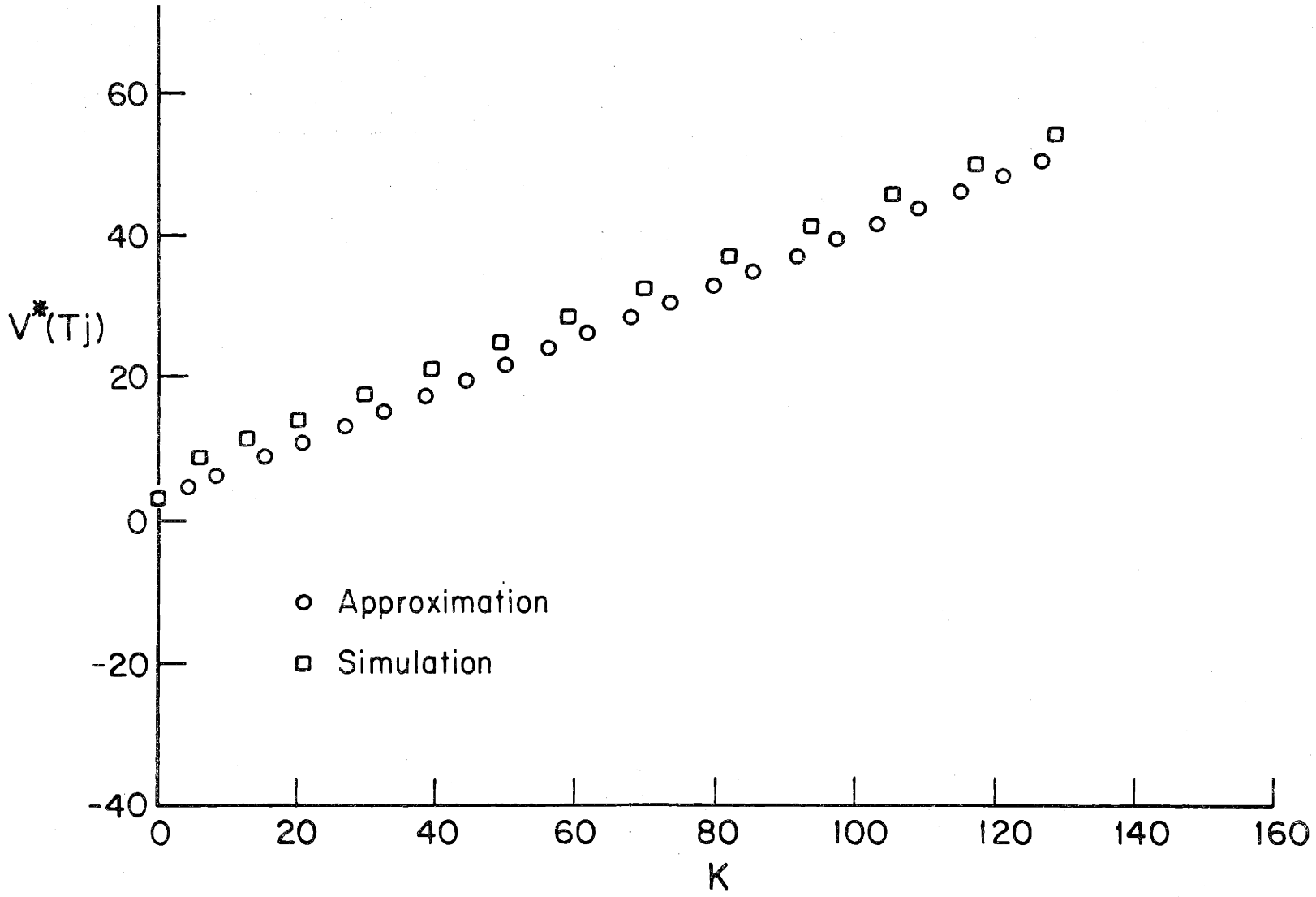

Figure 2.4c $V^*(T_j)$ for Simulation and Approximation

states at these times. Even with these inaccuracies, the approximation is still useful in predicting the type of response. Looking at the different cases, the accuracies of the approximation are seen.

For the hyperbolically stable case (1a), similarities are seen in the approximation and the simulation. First, the negative increment of V* for both the approximation and the system simulation indicates the system is stable. Secondly, the increment is nearly the same for both the approximation and simulation, indicating the degree of stability, rate of decay of the states, is quite similar. Thirdly, the time interval between switches in the probability is increasing with time, again a property of the approximation and the system response.

For the other two cases (1b, 1c) the approximation agrees with the system response in a similar manner, indicating the neutral stability and instability, respectively, and the change in switch times intervals for the probability with good accuracy.

From these examples, some conclusions can be drawn concerning the utility of this approximate analysis. In the examination of the qualitative behavior of the MMAC, this approximation would be useful. The insights gained in Greene's worst case analysis using this approximation demonstrate its usefulness. The explicit indication of stability and switch time trends are useful in understanding the response of a MMAC system. It should be noted that the qualitative accuracy is good, but the quantitative accuracy is not nearly as good. As with most approximation, however, some care must be taken in using this method to ensure no assumptions vital to the approximation accuracy are violated.

For example, later, in Section 2.3, the effect of violating the assumption that $P \simeq 0$ or $P \simeq 1$ on the accuracy of the approximation is investigated.

2.3 Limited Memory MMAC

One of the properties exhibited in the case of hyperbolic oscillations is the large excursions of the state as they are alternately stabilized and destabilized. Greene [6] showed this is mainly due to the inertia or lag in the probabilities. Since the probabilities are based on all past observations, the probabilities may be driven toward 0 (or 1) during one time interval, and then have to overcome the inertia of the prior interval to reverse direction and go to 1 (or 0). This is illustrated in the log likelihood formulation of the MMAC, repeated here.

$$\alpha(k+1) = \alpha(k) + \|\underline{r}_1(k+1)\|^2_{\underline{\theta}_1^{-1}} - \|\underline{r}_2(k+1)\|^2_{\underline{\theta}_2^{-1}} \tag{1.25}$$

$$P(k) = \left(1 + \frac{1 - P_0}{P_0}\, \beta \exp(-\tfrac{1}{2}\alpha(k))\right)^{-1} \tag{1.26}$$

$$\beta = \sqrt{|\underline{\theta}_1|\ |\underline{\theta}_2|}$$

In this case, $\alpha(k)$ tends to attain large values compared to the increment $\Delta\alpha(k)$ defined as follows:

$$\Delta\alpha(k) = \|\underline{r}_1(k+1)\|^2_{\underline{\theta}_1^{-1}} - \|\underline{r}_2(k+1)\|^2_{\underline{\theta}_2^{-1}} \tag{2.37}$$

so if $\alpha(k)$ gets large in the positive sense compared to $\Delta\alpha(k)$, it will take many times steps before $\alpha(k)$ is reduced to zero by a sequence of

negative increments. During this interval the unstable states will grow geometrically, resulting in the peaks seen at the switch times of the probability.

A modification to the MMAC proposed by Greene to "speed up the probabilities" or reduce the inertia is to limit the memory of the MMAC. This is done by introducing a moving observation window for the computation of the probabilities, i.e., instead of using all past observations for the computation of the probabilities, only the most recent observations are used [6]. For the log likelihood formulation, only the equation for $\alpha(k)$ (2.14) is changed in implementing the limited memory MMAC algorithm. For an observation window of length M, the equation for $\alpha(k)$ is as follows:

$$\alpha(k) = \sum_{i=k-M}^{k} \|\underline{r}_1(i)\|^2_{\underline{\theta}_1^{-1}} - \|\underline{r}_2(i)\|^2_{\underline{\theta}_2^{-1}} \tag{2.38}$$

A limiting case of the limited memory MMAC algorithm is where the probabilities are based on only the last observation. In this case equation (2.38), a dynamic equation for $\alpha(k)$, becomes a static equation

$$\alpha(k) = \|\underline{r}_1(k)\|^2_{\underline{\theta}_1^{-1}} - \|\underline{r}_2(k)\|^2_{\underline{\theta}_2^{-1}} \tag{2.39}$$

To obtain some insights into the behavior of the system, an approximation similar to that for the full memory MMAC is derived in this section. For the limited memory case, the equation for $\alpha(k)$ in terms of $\underline{y}_1(k)$, $\underline{y}_2(k)$, σ_1, and σ_2, defined in (2.3), (2.24) - (2.25) is:

$$\alpha(k) \simeq \|\underline{y}_1(k)\|^2\sigma_1 - \|\underline{y}_2(k)\|^2\sigma_2 \tag{2.40}$$

With this formulation, the half period T, defined in equation (2.29), can be approximated, assuming P(k) switches between zero and one, and does not take on intermediate values. Assuming $P(k) = 0$ on the interval $[T_j, T_{j+1})$, then it follows from the assumptions on $\underline{y}_1(k)$ and $\underline{y}_2(k)$ (Section 2.1):

$$\|\underline{A}_1(0)\|^2 = a_1 > 1 \tag{2.41}$$

$$\|\underline{A}_2(0)\|^2 = a_2 < 1 \tag{2.42}$$

Approximating $\|\underline{r}_i(T_j+k)\|^2_{\underline{\theta}_i} - 1$ by $a_i^k \|\underline{y}_i(T_j)\|^2 \sigma_i$ on this interval, simplifies the analysis and results in

$$\alpha(k+T_j) = a_1^k \|\underline{y}_1(T_j)\|^2 \sigma_1 - a_2^k \|\underline{y}_2(T_j)\|^2 \sigma_2 \tag{2.43}$$

If

$$\|\underline{y}_1(T_j)\|^2 < \|\underline{y}_2(T_j)\|^2 \tag{2.28}$$

and

$$\alpha(T_{j+1}) \simeq 0 \tag{2.27}$$

then T can be approximated by the following equation.

$$0 = a_1^T \|\underline{y}_1(T_j)\|^2 \sigma_1 - a_2 \|\underline{y}_2(T_j)\|^2 \sigma_2 \tag{2.44}$$

This equation can be solved for T, resulting in the following.

$$T = \frac{1}{(\ln a_1 - \ln a_2)} \ln \left(\frac{\|\underline{y}_2(T_j)\|^2 \sigma_2}{\|\underline{y}_1(T_j)\|^2 \sigma_1} \right) \tag{2.45}$$

Three cases were used to evaluate the approximation and simultaneously investigate the properties of the limited memory MMAC. The cases are the same used to check the full memory approximation and are defined in Table 2.1. Figures 2.5a, 2.5b, and 2.5c contrast the behavior predicted by the approximation with the simulation results.

One of the interesting properties of the approximation is that it predicts that the probability switches every time instant, after the first few switches. This is an erroneous prediction, since the minimum interval found in the simulations has a length of three time steps, but again the qualitative prediction is correct. In terms of the prediction of stability, the approximation correctly predicts the rate of growth for the neutrally stable hyperbolic case (2b) and the unstable hyperbolic case (2c). For the limited memory implementation hyperbolically stable system case (2a), the norms of the states $||\underline{y}_1(k)||^2$ and $||\underline{y}_2(k)||^2$ are predicted to decrease to zero, but the simulation exhibits a limit cycle type response.

The limit cycle response of the simulation can be explained as follows. As the norm of the states, $||\underline{y}_1(k)||^2$ and $||\underline{y}_2(k)||^2$ decrease toward zero, the probability will move toward ½. For P(k) fixed at ½, the system is unstable, and so as P(k) approaches ½, the system becomes unstable, or the norms $||\underline{y}_1(k)||^2$ and $||\underline{y}_2(k)||^2$ increase. This increase in these norms drives P(k) away from ½, towards 0 or 1. This shifting of P(k) from 0 or 1 to near ½ and back leads to the limit cycle type behavior.

An assumption made in the derivation of this approximation was that P(k) was either 0 or 1 and did not take on any intermediate values. In the simulation, P(k) did take on intermediate values as the system limit

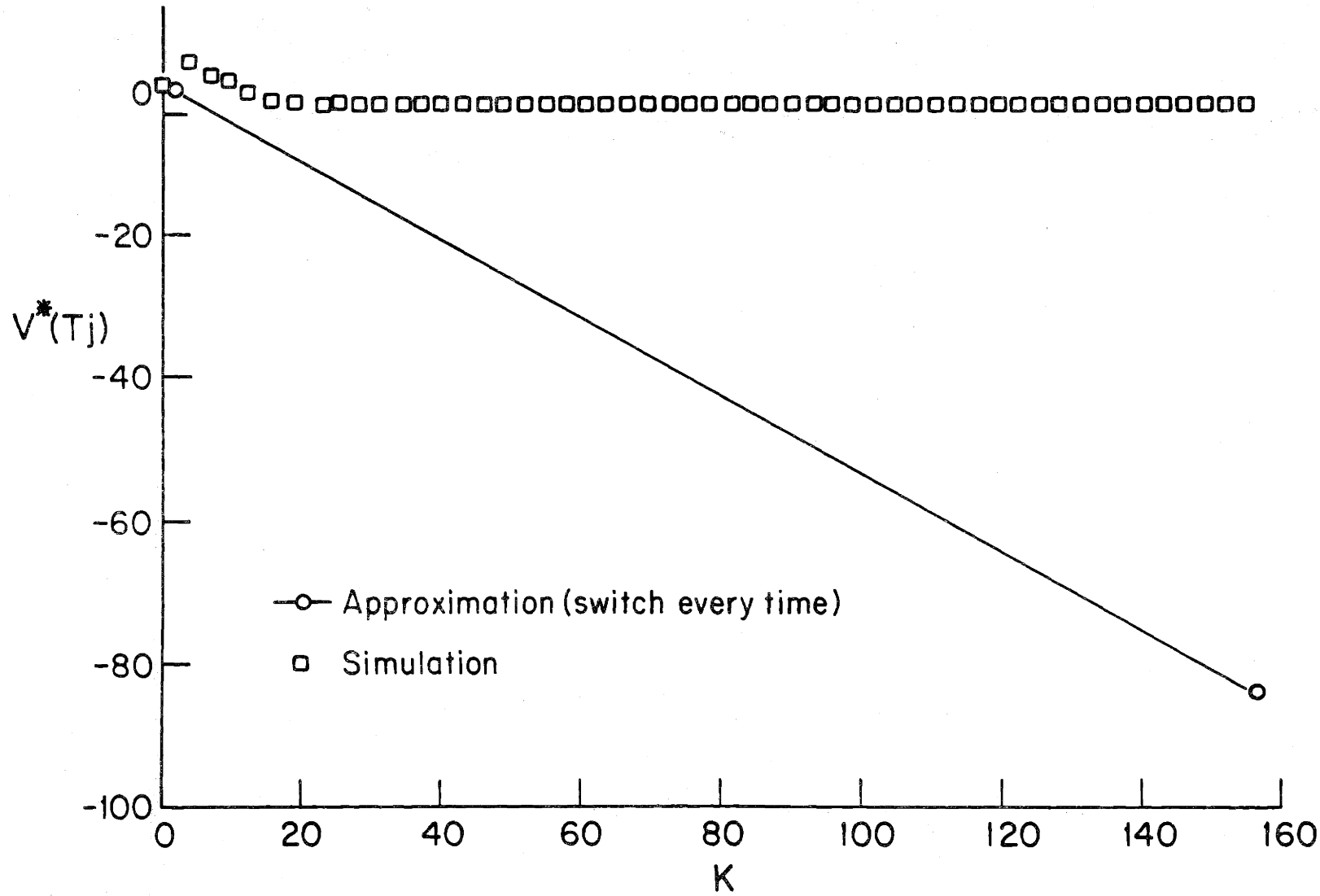

Figure 2.5a $V^*(T_j)$ for Simulation and Approximation (Limited Memory)

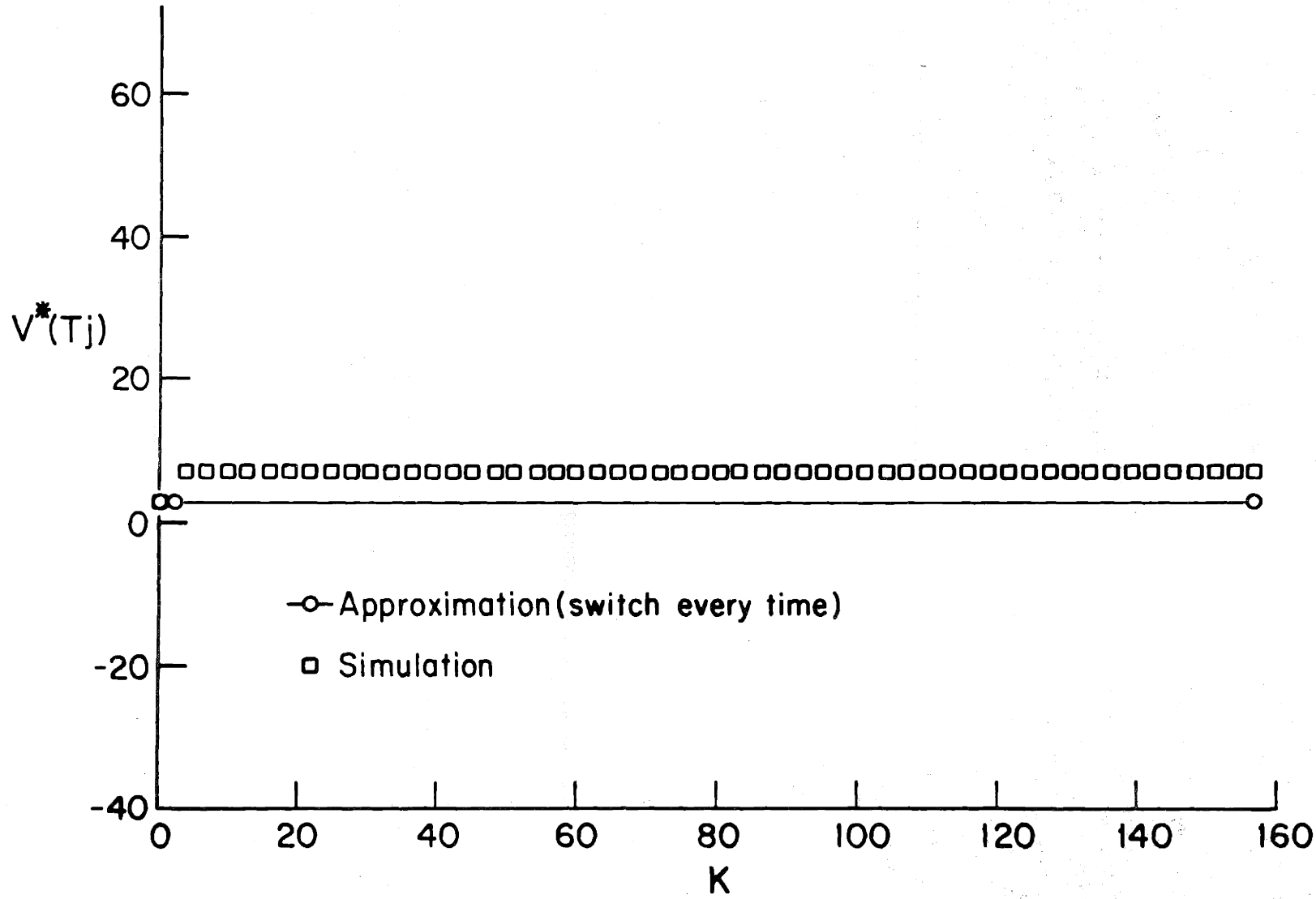

Figure 2.5b $V^*(T_j)$ for Simulation and Approximation (Limited Memory)

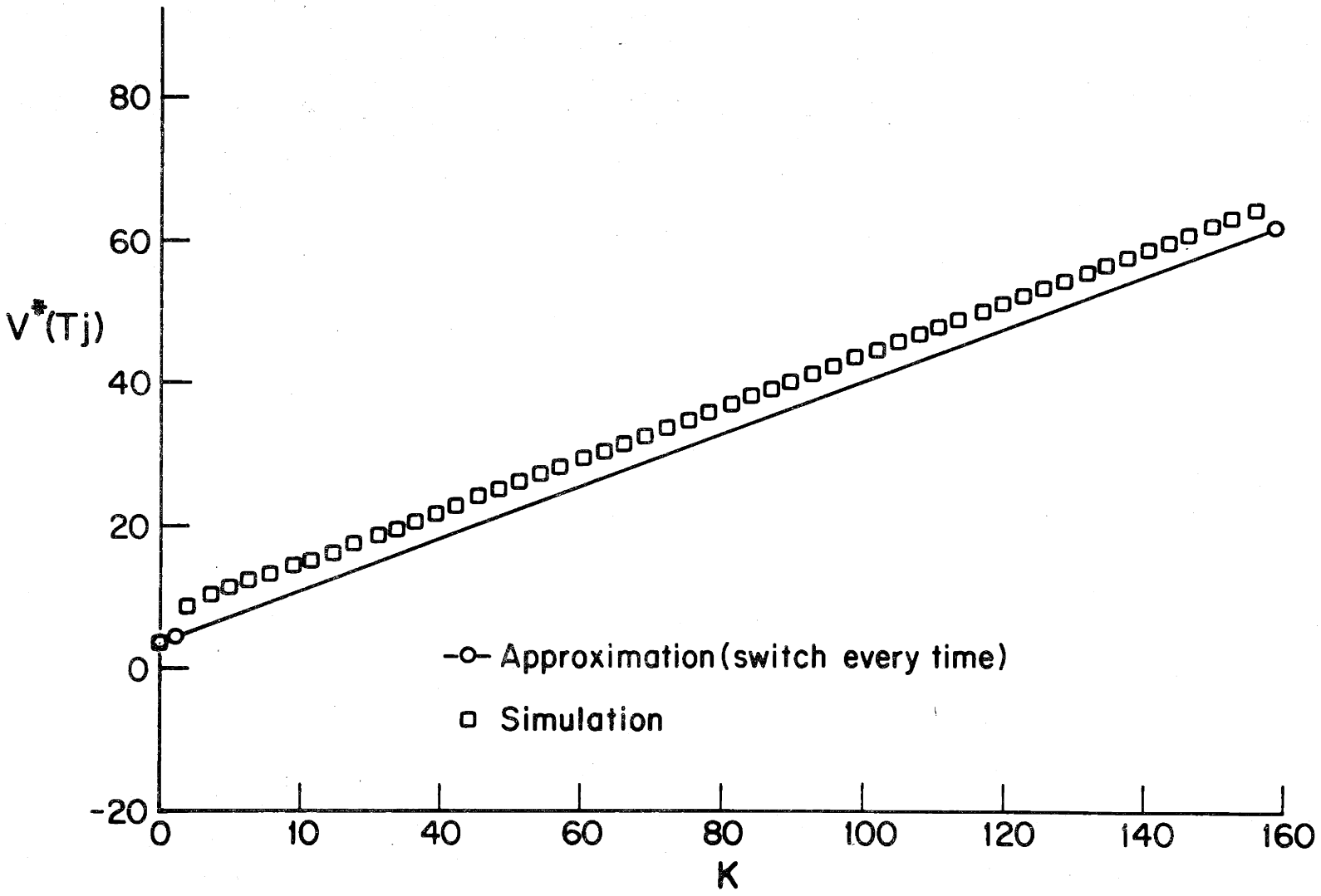

Figure 2.5c $V^*(T_j)$ for Simulation and Approximation (Limited Memory)

cycled violating the assumption. This explains the discrepancy between the approximation and the assumption.

An example of this type of limit cycle response is seen in Figure 2.5. For the initial portion of the time history ($0 \leqq k < 16$), the approximation and the simulation agree as to the stabilization of the states, but later in the time history ($k \geqq 16$) the stability indication of the approximation and the simulation differ. A look at P(k) for these two different intervals, ($0 \leqq k < 16$) and ($k \geqq 16$), reveals the cause of the discrepancy in the approximation and the simulations. In the initial interval, the values taken on by P(k) were essentially zero or one, but during the latter interval P(k) was near one-half. This violated the assumption that P(k) was near zero or one, resulting in a limit cycle.

A look at the initial conditions supports the claim of degradation to a limit cycle response.

$$\|\underline{y}_1(0)\|^2 = 100. \tag{2.46}$$

$$\|\underline{y}_2(0)\|^2 = 1. \tag{2.47}$$

For the initial switch intervals $\|\underline{y}_1(k)\|^2$ and $\|\underline{y}_2(k)\|^2$ were significantly different, due to the difference in the initial conditions. For later switch intervals, the state had been reduced so that the difference between them was small. At this point, $\alpha(k)$ was near zero, so the probability was near one-half, and not near zero or one, where some of the states would be stabilized. When the states reached nearly the same size, a limit cycle resulted.

To test the hypothesis that intermediate values of P(k) would account for the discrepancy in the simulation and the approximation, a maximum likelihood control was used instead of the probabilistically weighted control, i.e., the following control law was used.

$$\underline{u}(k) = \begin{cases} -\underline{G}_1\hat{\underline{x}}_1(k) & P(k) > \frac{1}{2} \\ -\underline{G}_2\hat{\underline{x}}_2(k) & P(k) < \frac{1}{2} \end{cases} \qquad (2.48)$$

In this case, the control is precisely piecewise linear, with gains corresponding to the P = 0 and P = 1 limits.

It was found that the negative increment of the quasi-Lyapunov function (V*(k)), indicative of the stability of the system, is exhibited by both the simulation and the approximation, i.e., the limit cycle was eliminated. Since the only change in the control was to ensure the assumption was valid, it would appear that P(k) taking on intermediate values in the probabilistically weighted control contributed to the neutral stability of the limited memory MMAC system.

The discrepancy between the approximation and the simulation for the hyperbolically stable case (2a) of the limited memory MMAC with probabilistically weighted control demonstrated an effect of violating the P(k) = 0 or P(k) = 1 assumption. The significance of the assumption is brought out, when in violating it, the approximation breaks down.

If the assumption of P(k) = 0 or P(k) = 1 is not violated, the approximation is fairly good. The prediction concerning the stability of the system appears to be correct, although care must be taken in the stable case. In the case of a prediction of stability, the actual system may limit cycle, as P(k) takes on intermediate values.

2.4 Set Point Analysis

In the analyses done thus far, the control associated with each model was designed to drive the state to the origin. In this section, an extension of this zero set point analysis is undertaken. The more general case of interest in this section is where the control associated with each model is biased.

$$\underline{u}_i(k) = -\underline{G}_i\hat{\underline{x}}_i(k) + \underline{b}_i \tag{2.49}$$

If the controller were linear, this bias would not affect the stability of the system, but since the MMAC is a nonlinear controller, the bias may affect the stability. It should be noted that the bias also affects the MMAC probabilities. If the Kalman filters used in the MMAC were all matched with the true system (plant), the bias would not affect the probabilities, but since there is no guarantee that all the filters are matched, the bias will affect the probabilities through the mis-matched Kalman filters.

To gain some insights into the effects of a biased control, an approximation was developed for the time between switches in the probability. As before, in this approximation the states are partitioned into those unstable for $P(k) = 0$, $\underline{y}_1(k)$ and $P(k) = 1$, $\underline{y}_2(k)$. With the assumption of a diagonal system, the equations for the evolution of $\underline{y}_1(k)$ and $\underline{y}_2(k)$ are:

$$\begin{bmatrix}\underline{y}_1(k+1)\\ \underline{y}_2(k+1)\end{bmatrix} = \begin{bmatrix}\tilde{\underline{A}}_1(P(k)) & 0\\ 0 & \tilde{\underline{A}}_2(P(k))\end{bmatrix}\begin{bmatrix}\underline{y}_1(k)\\ \underline{y}_2(k)\end{bmatrix} + \begin{bmatrix}\tilde{\underline{b}}_1(P(k))\\ \tilde{\underline{b}}_2(P(k))\end{bmatrix} \tag{2.50}$$

where $\tilde{\underline{A}}_1(P(k))$ and $\tilde{\underline{A}}_2(P(k))$ are defined by equation (2.3) and $\tilde{\underline{b}}_1(P(k))$, $\tilde{\underline{b}}_2(P(k))$ are appropriately partitioned versions of $(P(k)\underline{b}_1 + (1 - P(k)\underline{b}_2)$.

To compute the half period T, (2.29), assume a switch-like behavior in P(k), and that P(k) = 0 for the interval $[T_j, T_{j+1})$. The evolution of $\|\underline{y}_1(k)\|^2$ and $\|\underline{y}_2(k)\|^2$ can be approximated by the following equations.

$$\|\underline{y}_1(T_j+k)\|^2 = (d_1^k\|\underline{y}_1(T_j)\| + \frac{d_1^k - 1}{d_1 - 1}\|\tilde{\underline{b}}_1(0)\|)^2 \tag{2.51}$$

$$\|\underline{y}_2(T_j+k)\|^2 = (d_2^k\|\underline{y}_2(T_j)\| + \frac{d_2^k - 1}{d_2 - 1}\|\tilde{\underline{b}}_2(0)\|)^2 \tag{2.52}$$

Using these two approximations (2.51) - (2.52) in the equation for $\alpha(k)$, the following approximation for the evolution of $\alpha(k)$ is obtained.

$$\alpha(k) = \alpha(T_j) + \sum_{i=0}^{k}(d_1^i\|\underline{y}(T_j)\| + \frac{d_1^i - 1}{d_1 - 1}\|\tilde{\underline{b}}_1(0)\|)^2\sigma_1 - (d_2^i\|\underline{y}(T_j)\| + \frac{d_2^i - 1}{d_2 - 1}\|\tilde{\underline{b}}_2(0)\|)^2\sigma_2 \tag{2.53}$$

where

$$d_1 = \max|\lambda(\tilde{\underline{A}}_1(0))| \tag{2.54}$$

$$d_2 = \max|\lambda(\tilde{\underline{A}}_2(0))| \tag{2.55}$$

Now if

$$\alpha(T_j) \simeq 0 \tag{2.56}$$

$$\alpha(T_{j+1}) \simeq 0 \tag{2.57}$$

$$\|\underline{y}_1(T_j)\|^2 < \|\underline{y}_2(T_j)\|^2 \tag{2.58}$$

The time interval between switches T can be approximated using the following:

$$\sum_{k=0}^{T} \left(d_1^k \|\underline{y}_1(T_j)\| + \frac{d_1^k - 1}{d_1 - 1} \|\tilde{\underline{b}}_1(0)\|\right)^2 \simeq \sum_{k=0}^{T} \left(d_2^k \|\underline{y}_2(T_j)\| + \frac{d_2^k - 1}{d_2 - 1} \|\tilde{\underline{b}}_2(0)\|\right)^2 \tag{2.59}$$

or equivalently,

$$\left\{ \left[\frac{d_1^{2(T+1)} - 1}{d_1 - 1}\right] \|\underline{y}_1(T_j)\|^2 + \frac{2}{(d_1-1)(d_1^2-1)} (d_1^{2(T+1)} - d_1^{T+2} - d_1^{T+1} + d_1) \|\underline{y}_1(T_j)\| \|\tilde{\underline{b}}_1(0)\| \right.$$

$$\left. + \frac{1}{(d_1-1)^2} \left[\frac{1}{d_1^2-1} (d_1^{2(T+1)} - 2d_1^{T+2} - 2d_1^{T+1} + 2d_1 + 1) + T + 1 \right] \|\tilde{\underline{b}}_1(0)\|^2 \right\} \sigma_1$$

$$\simeq \left\{ \left[\frac{d_2^{2(T+1)} - 1}{d_2 - 1}\right] \|\underline{y}_2(T_j)\|^2 + \frac{2}{(d_2-1)(d_2^2-1)} (d_2^{2(T+1)} - d_2^{T+2} - d_2^{T+1} + d_2) \|\underline{y}_2(T_j)\| \|\tilde{\underline{b}}_2(0)\| \right.$$

$$\left. + \frac{1}{(d_2-1)^2} \left[\frac{1}{d_2^2-1} (d_2^{2(T+1)} - 2d_2^{T+2} - 2d_2^{T+1} + 2d_2 + 1) + T + 1 \right] \|\tilde{\underline{b}}_2(0)\|^2 \right\} \sigma_2 \tag{2.60}$$

Assuming

$$d_1 > 1 \tag{2.61}$$

$$d_2 < 1 \tag{2.62}$$

and consequently, for large T

$$d_1^T \gg d_1 \tag{2.63}$$

$$d_2^T \ll d_2 \tag{2.64}$$

then (2.60) reduces to the following:

$$\left[\left(\frac{d_1^{2(T+1)}}{d_1^2-1}\right)\|\underline{y}_1(T_j)\|^2 + 2\frac{d_1^{2(T+1)}}{(d_1^2-1)(d_1-1)}\|\underline{y}_1(T_j)\|\,\|\tilde{\underline{b}}_1(0)\| + \frac{1}{(d_1^2-1)}\frac{d_1^{2(T+1)}}{(d_1^2-1)}\|\tilde{\underline{b}}_1(0)\|^2\right]\sigma_1$$

$$\simeq \left[\left(\frac{1}{1-d_2^2}\right)\|\underline{y}_2(T_j)\|^2 + 2\frac{d_2}{(1-d_2)(1-d_2^2)}\|\underline{y}_2(T_j)\|\,\|\tilde{\underline{b}}_2(0)\| + \frac{T+1}{(d_2-1)^2}\|\tilde{\underline{b}}_2(0)\|^2\right]\sigma_2 \tag{2.65}$$

After some simplification, the equation (2.65) reduces to the following, which is used to approximate T.

$$\frac{d_1^{2(T+1)}\sigma_1}{(d_1^2-1)}\left(\|\underline{y}_1(T_j)\| + \frac{1}{d_1-1}\|\tilde{\underline{b}}_1(0)\|\right)^2$$

$$\simeq \frac{\sigma_2}{1-d_2^2}\left[\|\underline{y}_2(T_j)\|\left(\|\underline{y}_2(T_j)\| + \frac{2d_2}{1-d_2}\|\tilde{\underline{b}}_2(0)\|\right) + \frac{1+d_2}{1-d_2}\|\tilde{\underline{b}}_2(0)\|^2\right] \tag{2.66}$$

The stability of the system can be determined in a way analogous to Greene. The relative size of the peaks at the switch time can be determined using the following equivalent form of equation (2.66):

$$\|\underline{y}_1(T_{j+1})\|^2 \simeq \frac{\sigma_2}{\sigma_1}\frac{d_1^2-1}{d_2^2(d_2^2-1)}\left[\|\underline{y}_2(T_j)\|^2+\left(\frac{2d_2}{1-d_2}\|\underline{y}_2(T_j)\|+\frac{1-d_2^2}{(d_2-1)^2}(T+1)\|\tilde{\underline{b}}_2(0)\|\right)\|\tilde{\underline{b}}_1(0)\|\right] \tag{2.67}$$

For the case where $\|\tilde{\underline{b}}_i(0)\| = 0$, this equation reduces to the zero set point equation used by Greene [6]. In the case of interest in this section, $\|\tilde{\underline{b}}_i(0)\|$ is not zero, and equation (2.67) must be used. Due to the complexity of the equation (2.67) no simple condition, involving the parameters of the MMAC system, has been developed for the stability of the nonzero set point MMAC system.

Before recommending that the approximation derived in this section be used in any future work, an analysis of its accuracy is desired. A check of the accuracy of this approximation was done for the three cases defined in Table 2.1. The bias in the control associated with each model was such that the desired equilibrium point for the plant states was the same.

$$x_{\text{steady state}} = \begin{bmatrix} 1. \\ 1. \end{bmatrix} \tag{2.68}$$

Insight into the behavior of the set point control was gained from the test cases investigated. All three cases were found to be unstable, even the hyperbolically stable case (3a). This would seem to indicate a need for a stronger stability condition for the nonzero set point control MMAC system than for the zero set point system.

A comparison of the approximation to the simulation results reveals the significantly better accuracy of this approximation compared to earlier

approximations investigated (Sections 2.2 and 2.3). The approximation derived in this section predicted the switch times with good accuracy and the magnitude of the states at these times was also predicted well, as seen in Figures 2.6a, 2.6b, and 2.6c. It is conjectured that the biased control inputs greatly accentuate the effects of the model mismatch, which would lead to a better approximation for the biased control case. It would seem that this approximation would be useful in future work concerning stability conditions for the nonzero set point MMAC system.

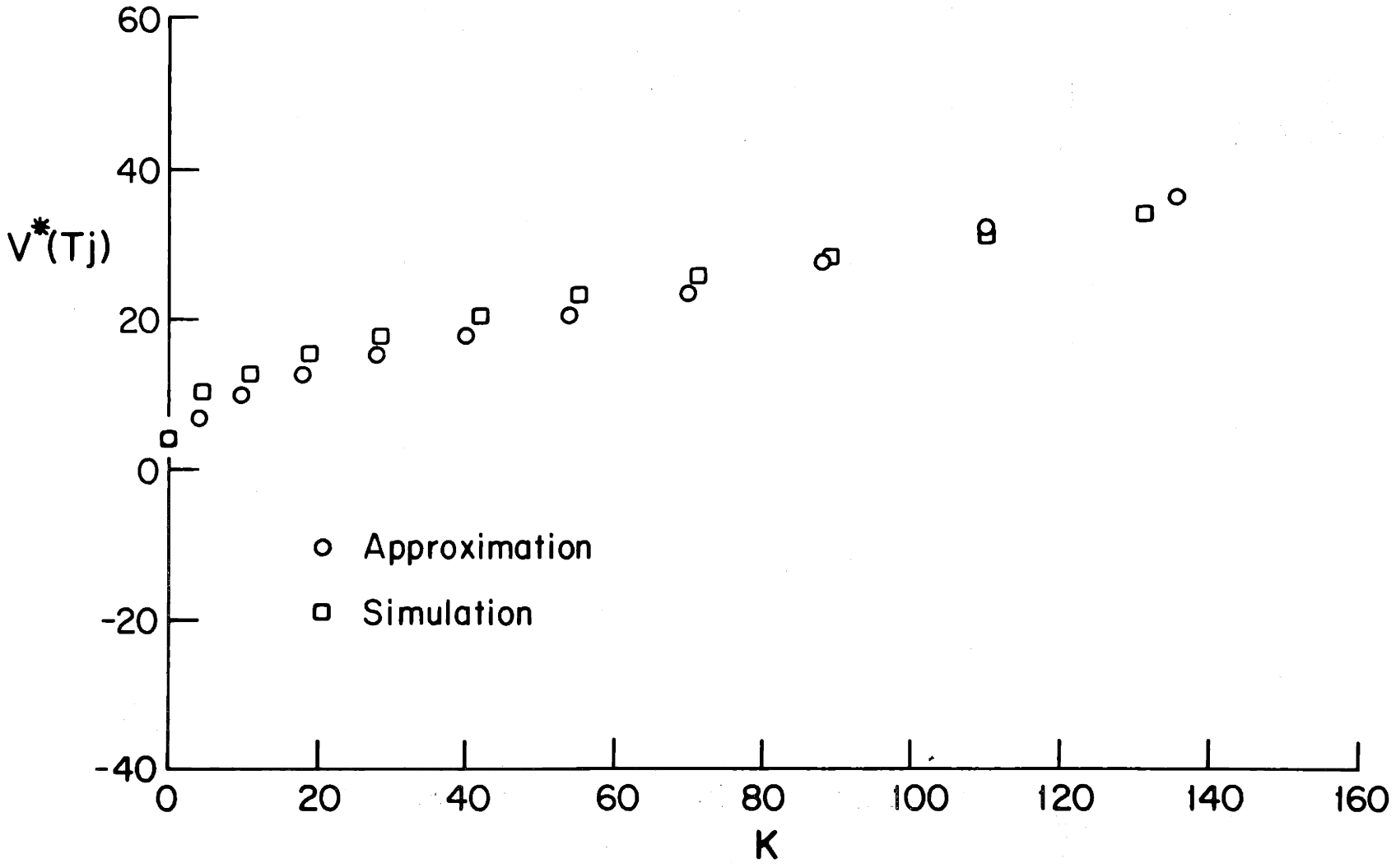

Figure 2.6a $V^*(T_j)$ for Simulation and Approximation (Set Point)

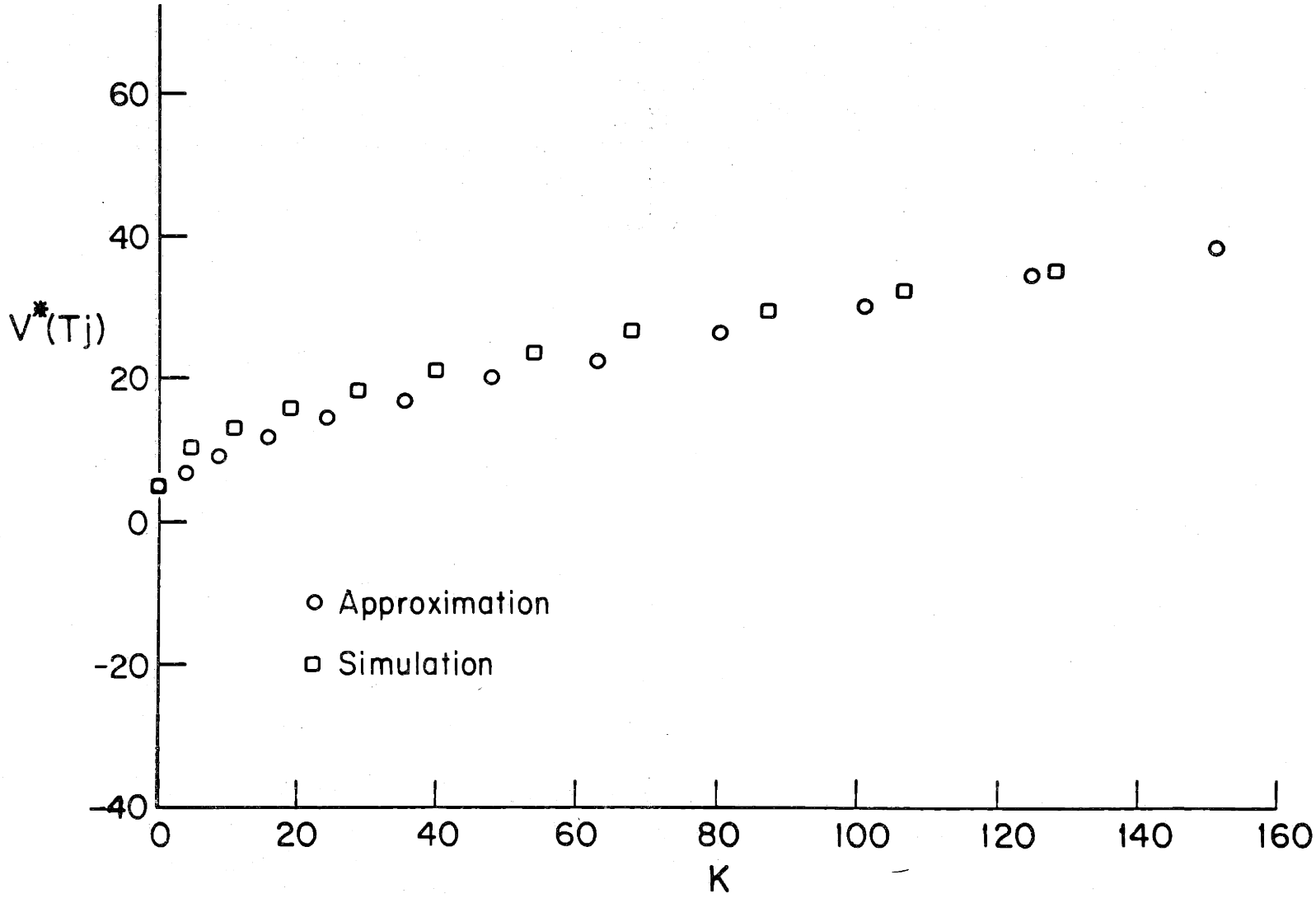

Figure 2.6b $V^*(T_j)$ for Simulation and Approximation (Set Point)

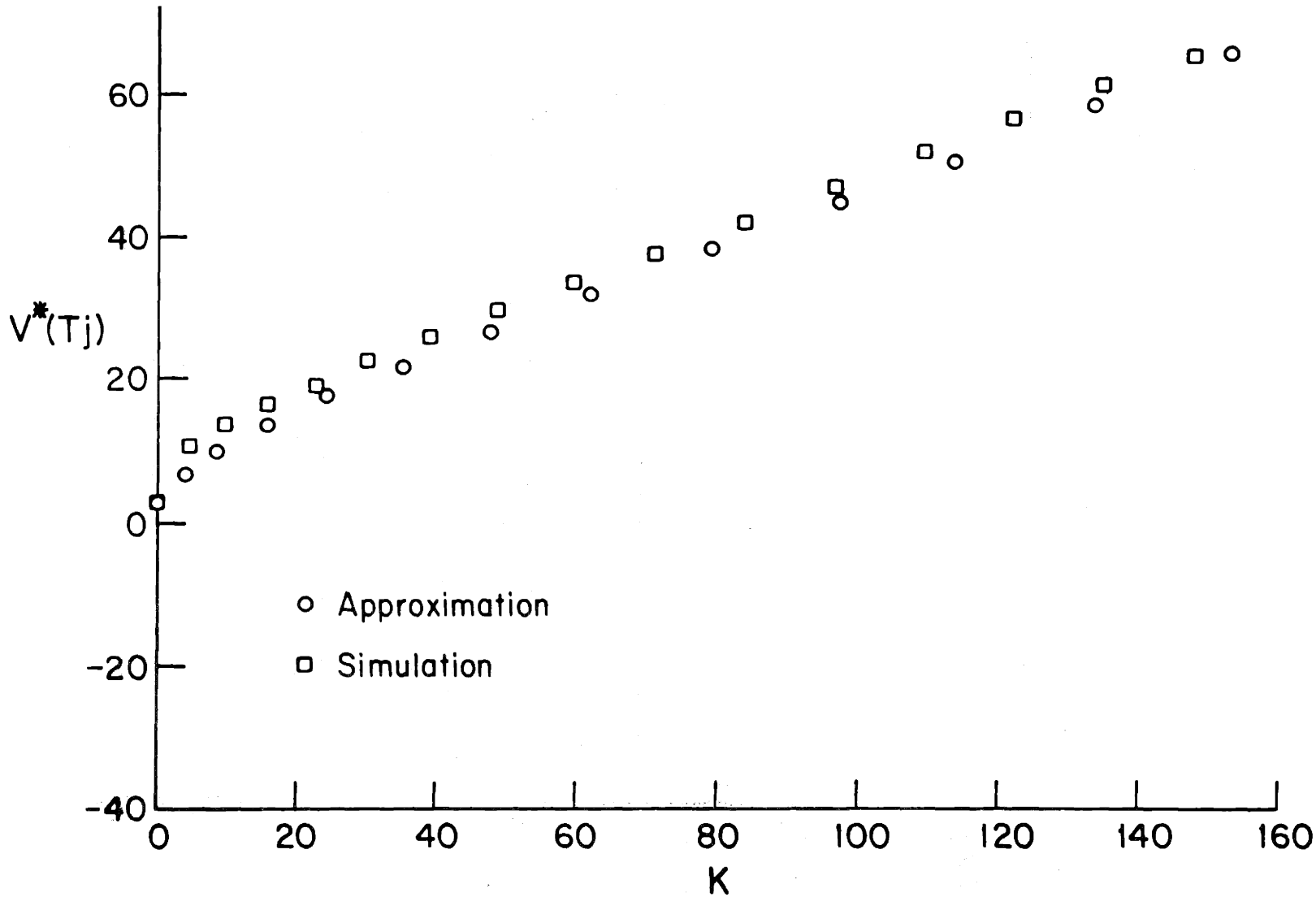

Figure 2.6c $V^*(T_j)$ for Simulation and Approximation (Set Point)

CHAPTER 3

STOCHASTIC ANALYSIS

This chapter is a presentation of the results of research into the stochastic properties of the MMAC. These results were obtained from a combination of exact and approximate analysis and simulations. This work constitutes a first step towards understanding the stochastic properties of the MMAC algorithm.

In Greene's work [6] and the work of the preceding chapter, the assumption of zero noise input was made. This simplifying assumption allowed many insights to be gained into the response of the deterministic MMAC. To obtain a complete understanding, the stochastic properties must also be investigated. Consequently, the noise sources have been assumed nonzero for the work in this chapter.

Since the MMAC is a nonlinear control algorithm, the analysis of the stochastic response is not straightforward. Even though the noise inputs are white and Gaussian, the nonlinearity leads to non-Gaussian probability densities for the states of the MMAC. These non-Gaussian densities impede the analysis by requiring numerical integration techniques for the Chapman-Kolmogorov equation [7].

A way of bypassing some of the difficulties of analyzing nonlinear stochastic systems is to use a quasi-linear approximation. One analysis of this type is a Random Input Describing Function (RIDF) approximation, which in its standard form leads to approximations for the first two moments

of the system states. The accuracy of this type of approximation varies significantly with different applications, i.e., sometimes it works, and sometimes it doesn't.

In Section 3.1, the RIDF method is outlined for a general nonlinear system. This section serves as the background for Section 3.2, where a RIDF is derived for the MMAC system. In Section 3.3, the concept of stable probability intervals is introduced as a way of classifying stochastic MMAC systems. In addition, this classification is compared to Greene's classifications for deterministic systems. To check the accuracy of the RIDF approximation, a set of test cases, defined in Section 3.4, are used in Monte Carlo simulations of the MMAC system. The results of these simulations are analyzed and compared to the predictions of the RIDF approximation in Section 3.5.

3.1 Random Input Describing Function

In the analysis of nonlinear stochastic systems, one technique for approximating the first two moments of the states of the system is the random input describing function (RIDF) [8]. This approximation has good accuracy for a large class of nonlinear equations. For this reason, the RIDF approximation was used in this analysis of the stochastic MMAC.

The basic idea of RIDF analysis is to develop a quasi-linear approximation for the nonlinearities in the system. This is done by computing minimum mean square error linear approximations for the nonlinearities, assuming an input of known distribution, usually Gaussian. For example, if

$$\underline{x}(k+1) = \underline{f}(\underline{x}(k)) + \underline{w}(k)$$
$$\underline{w}(k) \simeq N(\underline{0},\underline{w}) \tag{3.1}$$
$$E[\underline{w}(k)\underline{w}'(j)] = 0 \qquad j \neq k$$

A quasi-linear approximation can be computed as follows. Assuming

$$\underline{x}(k) \simeq N(\underline{m}(k),\underline{\Sigma}(k)) \tag{3.2}$$

then $\underline{f}(\cdot)$ can be approximated by

$$\hat{\underline{f}}(x(k)) = \underline{F}(\underline{m}(k),\underline{\Sigma}(k))(\underline{x}(k) - \underline{m}(k)) + \underline{b}(\underline{m}(k),\underline{\Sigma}(k)) \tag{3.3}$$

where $\underline{F}(\underline{m}(k),\underline{\Sigma}(k))$ and $\underline{b}(\underline{m}(k),\underline{\Sigma}(k))$ have been chosen to minimize

$$P = E\{[\underline{f}(\underline{x}(k)) - \underline{F}(\underline{m}(k),\underline{\Sigma}(k))(\underline{x}(k) - \underline{m}(k)) - \underline{b}(\underline{m}(k),\underline{\Sigma}(k))]$$
$$\times [\underline{f}(\underline{x}(k)) - \underline{F}(\underline{m}(k),-\underline{\Sigma}(k))(\underline{x}(k) - \underline{m}(k)) - \underline{b}(\underline{m}(k),\underline{\Sigma}(k)]\} \tag{3.4}$$

Once the functions $\underline{F}(\cdot,\cdot)$ and $\underline{b}(\cdot,\cdot)$ have been determined, the following equations can be used to approximate the evolution of the mean, $\hat{\underline{m}}(k)$, and the covariance, $\hat{\underline{\Sigma}}(k)$, of the system.

$$\hat{\underline{m}}(k+1) = \underline{b}(\hat{\underline{m}}(k),\hat{\underline{\Sigma}}(k)) \tag{3.5}$$
$$\hat{\underline{\Sigma}}(k+1) = \underline{F}(\hat{\underline{m}}(k),\hat{\underline{\Sigma}}(k))\hat{\underline{\Sigma}}(k)\underline{F}(\underline{m}(k),\bar{\underline{\Sigma}}(k)) + W \tag{3.6}$$

The reason for assuming that x(k) is Gaussian is twofold. First, the driving noise, w(k), is white and Gaussian implying that $\underline{x}(k)$ is always a convolution of a Gaussian and a non-Gaussian density. Secondly, and most important, the minimization of the error (3.4) is simplified, due to the moment factoring property of the Gaussian distribution. Whether this

assumption is reasonable depends upon the application.

The application of RIDF analysis to the MMAC system necessitates the linearization of the nonlinearities in the identification and control portions of the algorithm. The resulting quasi-linear system is used to approximate the means and covariances of the MMAC states.

3.2 Derivation of the RIDF for the MMAC System

In this section, a RIDF is derived for the two model MMAC system, defined in equations (1.18) - (1.27). This derivation approximates the nonlinearities in the identification and control sections of the algorithm, equations (1.24) - (1.27). The extension to the N-model MMAC, set point MMAC, etc. is conceptually straightforward.

The equation for the evolution of the log likelihood ratio $\alpha(k)$, (1.26), is quadratic in $\underline{r}_1(k)$ and $\underline{r}_2(k)$

$$\alpha(k+1) = \alpha(k) + \underline{r}_1'(k+1)\underline{\theta}_1^{-1}\underline{r}_1(k+1) - \underline{r}_2'(k+1)\underline{\theta}_2^{-1}\underline{r}_2(k+1) \qquad (3.7)$$

A RIDF for $\alpha(k+1)$ can be computed, assuming $\underline{r}_1(k)$ and $\underline{r}_2(k)$ are jointly Gaussian. Since the MMAC is a nonlinear controller, the plant states and filter estimates do not have Gaussian densities. The residuals, being functions of the states and filter estimates, are also non-Gaussian. To retain tractability in the computation of a RIDF for the MMAC, the residuals were assumed to be close to Gaussian. This assumption is reasonable, if there is substantial measurement noise. Under this assumption, $\alpha(k+1)$ can be approximated by the following.

$$\alpha(k+1) \simeq K_{\alpha\alpha}(\alpha(k) - m_\alpha(k)) + \underline{K}'_{\alpha r_1}(\underline{r}_1(k+1) - \underline{m}_{r_1}(k+1))$$

$$+ \underline{K}'_{\alpha r_2}(\underline{r}_2(k+1) - \underline{m}_{r_1}(k+1)) + \bar{b}_\alpha \qquad (3.8)$$

where $K_{\alpha\alpha}$, $\underline{K}_{\alpha r_1}$, $\underline{K}_{\alpha r_2}$, and b_α are functions of $\underline{m}_{r_1}(k+1)$, $\underline{m}_{r_2}(k+1)$, $\underline{\Sigma}_{r_1}(k+1)$, $\underline{\Sigma}_{r_2}(k+1)$ and $\Sigma_\alpha(k)$. After minimizing the expected error in the linearization, $K_{\alpha\alpha}$, $\underline{K}_{\alpha r_1}$, $\underline{K}_{\alpha r_2}$ and $\bar{b}_\alpha$ are defined as follows:

$$K_{\alpha\alpha} = 1 \qquad (3.9)$$

$$\underline{K}_{\alpha r_1} = 2\underline{\Sigma}_{r_1}(k+1)\underline{\theta}_1^{-1}\underline{m}_{r_1}(k+1) \qquad (3.10)$$

$$\underline{K}_{\alpha r_2} = -2\underline{\Sigma}_{r_2}(k+1)\underline{\theta}_2^{-1}\underline{m}_{r_2}(k+1) \qquad (3.11)$$

$$\bar{b}_\alpha = m_\alpha \qquad (3.12)$$

The RIDF approximation for this product of states type of nonlinearity has limitations. Geier [10] has proposed modifications to this method which improve the accuracy. His modified RIDF propagates higher order moments for those states used in the product nonlinearity. Later in this work, Section 3.5, as part of the analysis of the accuracy of the RIDF, it will be proposed that Geier's method be used to improve the accuracy of the approximation.

The states used in this analysis of the MMAC are the plant state, $\underline{x}(k)$, augmented by the filter estimates, $\hat{\underline{x}}_1(k)$ and $\hat{\underline{x}}_2(k)$, and by the log likelihood ratio $\alpha(k)$. To get the approximation for $\alpha(k+1)$ in terms of the state of the MMAC system, the following equalities are used:

$$\underline{r}_1(k+1) = \underline{A}\underline{x}(k) - \underline{A}_1\hat{\underline{x}}_1(k) + \underline{v}(k+1) + \underline{w}(k) \tag{3.13}$$

$$\underline{r}_2(k+1) = \underline{A}\underline{x}(k) = \underline{A}_2\hat{\underline{x}}_2(k) + \underline{v}(k+1) + \underline{w}(k) \tag{3.14}$$

Substituting for $\underline{r}_1(k+1)$ and $\underline{r}_2(k+1)$, using equations (3.13) - (3.14) in equation (3.7) the new approximation for $\alpha(k+1)$ is the following:

$$\begin{aligned}\alpha(k+1) = \alpha_k &+ \underline{K}'_{\alpha x}(\underline{x}(k) - \underline{m}_x(k)) + \underline{K}'_{\alpha\hat{x}_1}(\hat{\underline{x}}_1(k) - \underline{m}_{\hat{x}_1}(k)) \\ &+ \underline{K}'_{\alpha\hat{x}_2}(\hat{\underline{x}}_2(k) - \underline{m}_{\hat{x}_2}(k)) + \underline{K}'_{\alpha v}\underline{v}(k+1) + \underline{K}'_{\alpha w}\underline{w}(k1) + b_\alpha\end{aligned} \tag{3.15}$$

The functions $\underline{K}_{\alpha x}$, $\underline{K}_{\alpha\hat{x}_1}$, $\underline{K}_{\alpha\hat{x}_2}$, $\underline{K}_{\alpha v}$, $\underline{K}_{\alpha w}$, and b_α are defined as follows:

$$\underline{K}_{\alpha x} = 2\underline{A}'[\underline{\theta}_1^{-1}(\underline{A}\underline{m}_x(k) - \underline{A}_1\underline{m}_{\hat{x}_1}(k)) - \underline{\theta}_2^{-1}(\underline{A}\underline{m}_x(k) - \underline{A}_2\underline{m}_{\hat{x}_2}(k))] \tag{3.16}$$

$$\underline{K}_{\alpha\hat{x}_1} = 2\underline{A}_1'\underline{\theta}_1^{-1}(\underline{A}\underline{m}_x(k) - \underline{A}_1\underline{m}_{\hat{x}_1}(k)) \tag{3.17}$$

$$\underline{K}_{\alpha\hat{x}_2} = 2\underline{A}_2'(\underline{A}\underline{m}_x(k) - \underline{A}_2\underline{m}_{\hat{x}_2}(k)) \tag{3.18}$$

$$\underline{K}_{\alpha v} = 2[\underline{\theta}_1^{-1}(\underline{A}\underline{m}_x(k) - \underline{A}_1\underline{m}_{\hat{x}_1}(k)) - \underline{\theta}_2^{-1}(\underline{A}\underline{m}_x(k) - \underline{A}_2\underline{m}_{\hat{x}_2}(k))] \tag{3.19}$$

$$\underline{K}_{\alpha w} = \underline{K}_{\alpha v} \tag{3.20}$$

$$\begin{aligned}b_\alpha = \mathrm{tr}\{&\underline{\theta}_1^{-1}[\underline{A}\underline{\Sigma}_x(k)\underline{A}' - 2\underline{A}\underline{\Sigma}_{x\hat{x}_1}(k)\underline{A}_1' + \underline{A}_1\underline{\Sigma}_{\hat{x}_1}(k)\underline{A}_1' + \underline{V} + \underline{W} \\ &+ (\underline{A}\underline{m}_x(k) - \underline{A}_1\underline{m}_{\hat{x}_1}(k))(\underline{A}\underline{m}_x(k) - \underline{A}_1\underline{m}_{\hat{x}_1}(k))'] \\ &- \underline{\theta}_2^{-1}[\underline{A}\underline{\Sigma}_x(k)\underline{A}' - 2\underline{A}\underline{\Sigma}_{x\hat{x}_2}(k)\underline{A}_2' + \underline{A}_2\underline{\Sigma}_{\hat{x}_2}(k)\underline{A}_2' + \underline{V} + \underline{W} \\ &+ (\underline{A}\underline{m}_x(k) - \underline{A}_2\underline{m}_{\hat{x}_2}(k))(\underline{A}\underline{m}_x(k) - \underline{A}_1\underline{m}_{\hat{x}_2}(k))']\}\end{aligned} \tag{3.21}$$

For the nonlinearity defined by equations (1.24) - (1.25) the derivation of a describing function involved an expectation with the following term:

$$E\left[\left(\frac{1}{1+\beta\frac{1-P_0}{P_0}e^{\frac{\alpha(k)}{2}}}\right)\left(\underline{G}_1\underline{x}_1(k) - \underline{G}_2\hat{\underline{x}}_2(k)\right)\right]$$

where the expectation is taken over $\alpha(k)$, $\hat{\underline{x}}_1(k)$, and $\hat{\underline{x}}_2(k)$. The computation of this RIDF assumes $\alpha(k)$, $\hat{\underline{x}}_1(k)$ and $\hat{\underline{x}}_2(k)$ are jointly Gaussian. Even with this Gaussian assumption for the states an additional simplification is needed to compute the RIDF. To simplify the expectations involving this term and others similar to it, the following assumption was used.

$$\frac{1}{1+\beta\frac{1-P_0}{P_0}e^{\frac{\alpha(k)}{2}}} \simeq \left\{\begin{array}{ll} 1 & \alpha(k) > \alpha_{switch} \\ 0 & \alpha(k) < \alpha_{switch} \end{array}\right\} \tag{3.22}$$

$$\alpha_{switch} = 2 \ln \frac{P_0}{1-P_0}\beta \tag{3.23}$$

It should be noted that this approximation is precisely the maximum likelihood control formulation of the MMAC, defined in Section 2.3. Using this approximation (or exact expression, if the maximum likelihood control is used) (3.22) - (3.23), the describing function for equations (1.24) - (1.25) is the following.

$$u(k) = \underline{K}'_{ux}(\underline{x}(k) - \underline{m}_x(k)) + \underline{K}_{u\hat{x}_1}(\hat{\underline{x}}_1(k) - \underline{m}_{\hat{x}_1}(k)) + \underline{K}_{ux_2}(\hat{\underline{x}}_2(k) - \underline{m}_{\hat{x}_2}(k)) + \underline{K}_{u\alpha}(\alpha(k) - m_\alpha(k)) + \underline{b}_u \tag{3.24}$$

where the functions K_{ux}, $K_{u\hat{x}_1}$, $K_{u\hat{x}_2}$, $K_{u\alpha}$, and b_u are defined in the following equations.

$$\underline{K}_{ux} = \underline{0} \tag{3.25}$$

$$\underline{K}_{u\hat{x}_1} = q\underline{G}_1 \tag{3.26}$$

$$\underline{K}_{u\hat{x}_2} = (1-q)\underline{G}_2 \tag{3.27}$$

$$\underline{K}_{u\alpha} = -\frac{zf}{\Sigma_\alpha(k)}\left[\underline{G}_1\underline{\Sigma}_{\hat{x}_1\alpha}(k) - \underline{G}_2\underline{\Sigma}_{\hat{x}_2\alpha}(k)\right] - \frac{f}{\sqrt{\Sigma_\alpha(k)}}\left[\underline{G}_1\underline{m}_{\hat{x}_1}(k) - \underline{G}_2\underline{m}_{\hat{x}_2}(k)\right] \tag{3.28}$$

$$b_u = q\underline{G}_1\underline{m}_{\hat{x}_1}(k) + (1-q)\underline{G}_2\underline{m}_{\hat{x}_2}(k) - \frac{f}{\sqrt{\Sigma_\alpha(k)}}\left[\underline{G}_1\underline{\Sigma}_{\hat{x}_1\alpha}(k) - \underline{G}_2\underline{\Sigma}_{\hat{x}_2\alpha}(k)\right] \tag{3.29}$$

$$z = \frac{\alpha_{switch} - m_\alpha(k)}{\sqrt{\Sigma_\alpha(k)}} \tag{3.30}$$

$$f = \frac{1}{2\pi}\, e^{-z^2/2} \tag{3.31}$$

$$q = \int_{-\infty}^{z} \frac{1}{\sqrt{2\pi}}\, e^{-\lambda^2/2}\, d\lambda \tag{3.32}$$

This set of equations (3.15) - (3.21), (3.24) - (3.32) led to the following quasi-linear form for the MMAC.

$$\begin{bmatrix} \underline{x}(k+1) \\ \hat{\underline{x}}_1(k+1) \\ \hat{\underline{x}}_2(k+1) \\ \alpha(k+1) \end{bmatrix} \simeq \hat{\underline{A}}(k) \begin{bmatrix} \underline{x}(k) \\ \hat{\underline{x}}_1(k) \\ \hat{\underline{x}}_2(k) \\ \alpha(k) \end{bmatrix} + \hat{\underline{\Gamma}}(k) \begin{bmatrix} \underline{w}(k) \\ \underline{v}(k+1) \end{bmatrix} + \hat{\underline{B}}(k) \begin{bmatrix} \underline{m}_x(k) \\ \underline{m}_{\hat{x}_1}(k) \\ \underline{m}_{\hat{x}_2}(k) \\ m_\alpha(k) \\ \underline{b}_u(k) \\ b_\alpha(k) \end{bmatrix} \tag{3.33}$$

$$\hat{\underline{A}}(k) = \left[\begin{array}{cccc} \underline{A}-\underline{K}'_{ux} & -\underline{K}_{u\hat{x}_1} & -\underline{K}_{u\hat{x}_2} & -\underline{K}_{u\alpha} \\ \underline{H}_1\underline{A}-\underline{K}'_{ux} & (\underline{I}-\underline{H}_1)\underline{A}_1-\underline{K}'_{u\hat{x}_1} & -\underline{K}'_{u\hat{x}_2} & -\underline{K}_{u\alpha} \\ \underline{H}_2\underline{A}-\underline{K}'_{ux} & -\underline{K}_{u\hat{x}_1} & (\underline{J}-\underline{H}_2)\underline{A}_2-\underline{K}'_{u\hat{x}_2} & -\underline{K}_{u\alpha} \\ \underline{K}_{\alpha x} & \underline{K}'_{\alpha\hat{x}_1} & \underline{K}'_{\alpha\hat{x}_2} & \end{array}\right]\Bigg|_{\substack{\underline{m}_\cdot(\cdot)=\underline{m}_\cdot(k) \\ \underline{\Sigma}_\cdot(\cdot)=\underline{\Sigma}_\cdot(k)}} \tag{3.34}$$

$$\hat{\underline{\Gamma}}(k) \left[\begin{array}{cc} \underline{I} & 0 \\ \underline{H}_1 & \underline{H}_1 \\ \underline{H}_2 & \underline{H}_2 \\ \underline{K}'_{\alpha v} & \underline{K}'_{\alpha w} \end{array}\right]\Bigg|_{\substack{\underline{m}_\cdot(\cdot)=\underline{m}_\cdot(k) \\ \underline{\Sigma}_\cdot(\cdot)=\underline{\Sigma}_\cdot(k)}} \tag{3.35}$$

$$\hat{\underline{B}}(k) = \left[\begin{array}{cccccc} \underline{K}'_{ux} & \underline{K}'_{u\hat{x}_1} & \underline{K}'_{u\hat{x}_2} & \underline{K}_{u\alpha} & -\underline{I} & 0 \\ \underline{K}'_{ux} & \underline{K}'_{u\hat{x}_1} & \underline{K}'_{u\hat{x}_2} & \underline{K}_{u\alpha} & -\underline{I} & 0 \\ \underline{K}'_{ux} & \underline{K}'_{u\hat{x}_1} & \underline{K}'_{u\hat{x}_2} & \underline{K}_{u\alpha} & -\underline{I} & 0 \\ -\underline{K}'_{\alpha x} & \underline{K}'_{\alpha\hat{x}_1} & \underline{K}'_{\alpha\hat{x}_2} & 0 & 0 & 1 \end{array}\right]\Bigg|_{\substack{\underline{m}_\cdot(\cdot)=\underline{m}_\cdot(k) \\ \underline{\Sigma}_\cdot(\cdot)=\underline{\Sigma}_\cdot(k)}} \tag{3.36}$$

With this quasi-linear approximation, the approximations for the means and covariances of the MMAC system can be propagated in time using equations (3.37) - (3.40).

Let

$$\tilde{\underline{m}}(k) = E\begin{bmatrix} x(k) \\ \hat{x}_1(k) \\ \hat{x}_2(k) \\ \alpha(k) \end{bmatrix} \tag{3.37}$$

$$\tilde{\underline{\Sigma}}(k) = \text{cov}\left(\begin{bmatrix} x(k) \\ \dot{x}_1(k) \\ \dot{x}_2(k) \\ \alpha(k) \end{bmatrix}, \begin{bmatrix} x(k) \\ \dot{x}_1(k) \\ \dot{x}_2(k) \\ \alpha(k) \end{bmatrix} \right) \tag{3.38}$$

and $\hat{\tilde{\underline{m}}}(k)$, $\hat{\tilde{\underline{\Sigma}}}(k)$ be approximations for $\tilde{\underline{m}}(k)$, $\tilde{\underline{\Sigma}}(k)$. Then

$$\hat{\tilde{\underline{m}}}(k+1) = \hat{\underline{A}}(k)\hat{\tilde{\underline{m}}}(k+1) + \hat{\underline{B}}(k)\begin{bmatrix} \hat{\tilde{\underline{m}}}(k) \\ \hline b_u \\ b_\alpha \end{bmatrix} \tag{3.39}$$

$$\hat{\tilde{\underline{\Sigma}}}(k+1) = \hat{\underline{A}}(k)\hat{\tilde{\underline{\Sigma}}}(k)\hat{\underline{A}}'(k) + \hat{\underline{\Gamma}}(k)\begin{matrix} \underline{w} & 0 \\ 0 & \underline{v} \end{matrix}\hat{\underline{\Gamma}}'(k) \tag{3.40}$$

This approximation will be used later in this chapter, to demonstrate some of the properties of the stochastic MMAC system.

3.3 Stable Probability Intervals

In Greene's work, MMAC systems were classified according to the deterministic response. These classifications, universally stable, hyperbolic oscillations, and mixed case, lend themselves to equivalent classifications

for the stochastic MMAC. In this section, the idea of stable probability interval is used as a classification criterion. There is a direct correlation between Greene's classification and the stable probability interval classification, which is explained below.

As mentioned in Section 2.1, the MMAC system is linear for fixed P(k). The stability of the system can be determined for various values of P(k). The set of values of P(k) for which the MMAC system is stable is called the set of stable probabilities. In the cases of interest in this chapter, this set of stable probabilities defines an interval on [0,1], i.e.,

$$P_{stable} \in [P_{min}, P_{max}] \qquad 0 \leqq P_{min} \leqq P_{max} \leqq 1$$

For the work in Sections 3.5 - 3.7 the stable probability interval is an important quantity in determining the response of the stochastic MMAC. The following terminology is used in the discussions that follow:

1. Universally stable systems. These systems have a stable probability interval of [0,1].
2. End point stable intervals. These systems have a stable probability interval which includes 0 or 1.
3. Interior stable intervals. These systems have a stable interval which does not include 0 or 1.
4. No stable interval. These systems have no stable probability interval.

The following correlation exists between the stable probability interval and deterministic response characterizations.

Probability Interval		Deterministic Response
Universally stable	$\Longleftrightarrow$	Universally stable
End point and interior	$\Longleftrightarrow$	Mixed case
No stable interval	$\Longleftarrow$	Hyperbolic oscillations

There are systems with no stable probability interval that do not oscillate, i.e., the states grow without oscillatory behavior.

3.4 Case Definition

To illustrate the types of stochastic responses investigated, a few cases were chosen. These cases were used to check the accuracy of the RIDF, as well as to gain insight into the response characteristics. In this section background information for the case definition and Monte Carlo simulation is presented.

In the last section, the concept of stable probability interval was presented. In this section, the determination of cases with specified probability intervals is outlined. Also some motivation for the choice of cases is given.

To reduce the number of parameters which determine the stable probability interval, the following assumption was made.

$$Q = R = V = W = I \tag{3.41}$$

$$I = n \times n \text{ identity matrix} \tag{3.42}$$

With this simplification the matrices $\underline{A}$, $\underline{A}_1$, and $\underline{A}_2$ will determine the stable probability interval. The matrices $\underline{A}$, $\underline{A}_1$, and $\underline{A}_2$ being diagonal allows the following form.

$$\underline{A} = \begin{bmatrix} a & 0 \\ 0 & a \end{bmatrix} \tag{3.43}$$

$$\underline{A}_1 = \begin{bmatrix} a & 0 \\ 0 & a_1 \end{bmatrix} \tag{3.44}$$

$$\underline{A}_2 = \begin{bmatrix} a_2 & 0 \\ 0 & a \end{bmatrix} \tag{3.45}$$

$$\underline{H}_1 = \begin{bmatrix} h & 0 \\ 0 & h_1 \end{bmatrix} \tag{3.46}$$

$$\underline{H}_2 = \begin{bmatrix} h_2 & 0 \\ 0 & h \end{bmatrix} \tag{3.47}$$

$$\underline{G}_1 = \begin{bmatrix} g & 0 \\ 0 & g_1 \end{bmatrix} \tag{3.48}$$

$$\underline{G}_2 = \begin{bmatrix} g_2 & 0 \\ 0 & g \end{bmatrix} \tag{3.49}$$

$$\underline{\theta}_1 = \begin{bmatrix} 1+h & 0 \\ 0 & 1+h_1 \end{bmatrix} \tag{3.50}$$

$$\underline{\theta}_2 = \begin{bmatrix} 1+h_2 & 0 \\ 0 & 1+h \end{bmatrix} \tag{3.51}$$

where $\underline{H}_i$, $\underline{G}_i$ and $\underline{\theta}_i$ are obtained using equations (1.10) - (1.11), (1.13) - (1.14), (1.17), assuming $\underline{C}_i$ and $\underline{B}_i$ are identity matrices. In this case, the matrix equations (1.10) - (1.11), (1.13) - (1.14) can be replaced by the following set of independent scalar equations.

$$s_i = \frac{a_i^2}{2} + \sqrt{\left(\frac{a_i^2}{2}\right) + 1} \tag{3.52}$$

$$h_i = \frac{s_i}{s_i+1} \tag{3.53}$$

$$g_i = a_i h_i \tag{3.54}$$

Using this formulation, the matrices $\tilde{\underline{A}}_1(P)$ and $\tilde{\underline{A}}_2(P)$, defined by equation (2.3), reduce to the following form for this two state case.

$$\tilde{\underline{A}}_1(P) = \begin{bmatrix} a-Pg_1-(1-P)g_2 & P(1-h)g_1 & (1-P)(1-h_2)g_2 \\ 0 & (1-h_1)a & 0 \\ a-a_2 & 0 & (1-h_2)a_2 \end{bmatrix} \tag{3.55}$$

$$\tilde{\underline{A}}_2(P) = \begin{bmatrix} a-Pg_1-(1-P)g_2 & P(1-h_1)g_1 & (1-P)(1-h)g_2 \\ a-a_1 & (1-h_1)a_1 & 0 \\ 0 & 0 & (1-h)a \end{bmatrix} \tag{3.56}$$

These matrices $\tilde{\underline{A}}_1(P)$ and $\tilde{\underline{A}}_2(P)$, can be used to determine P_{min} and P_{max}, if they exist.

Using the Routh-Hurwitz criterion [9] to determine stable ranges for P, a plot of P_{min} as a function of a_2 for $\tilde{\underline{A}}_1(P)$ can be determined. An example of this plot, Figure 3.1, was made for the case where

$$a = 2.0 \tag{3.57}$$

An equivalent plot was also made for P_{max} as a function of a_1, Figure 3.2, for $\tilde{A}_2(P)$. For fixed a_1 and a_2, the stable probability interval is the

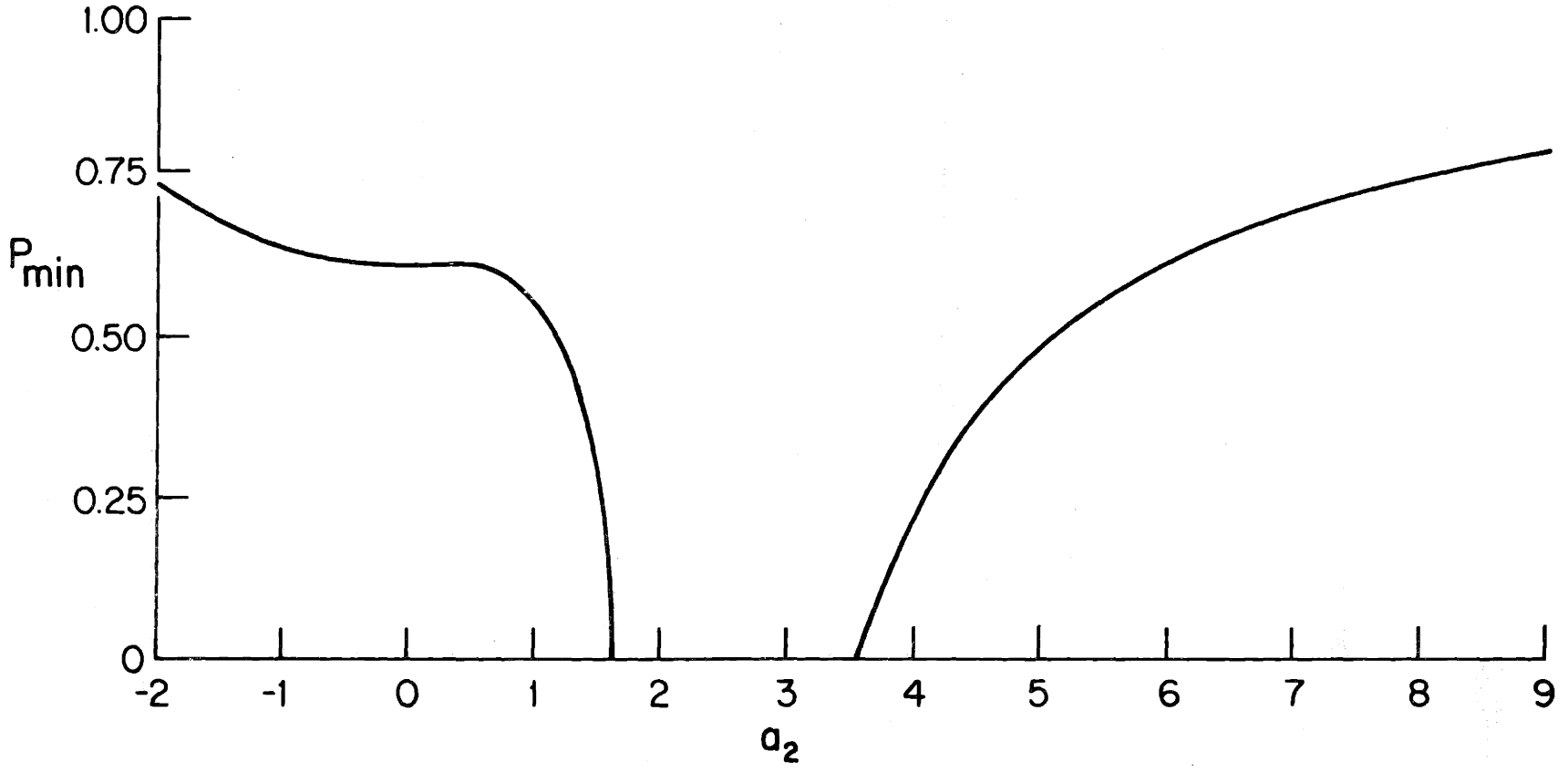

Figure 3.1 P_{min} vs. a_2 for a = 2.0

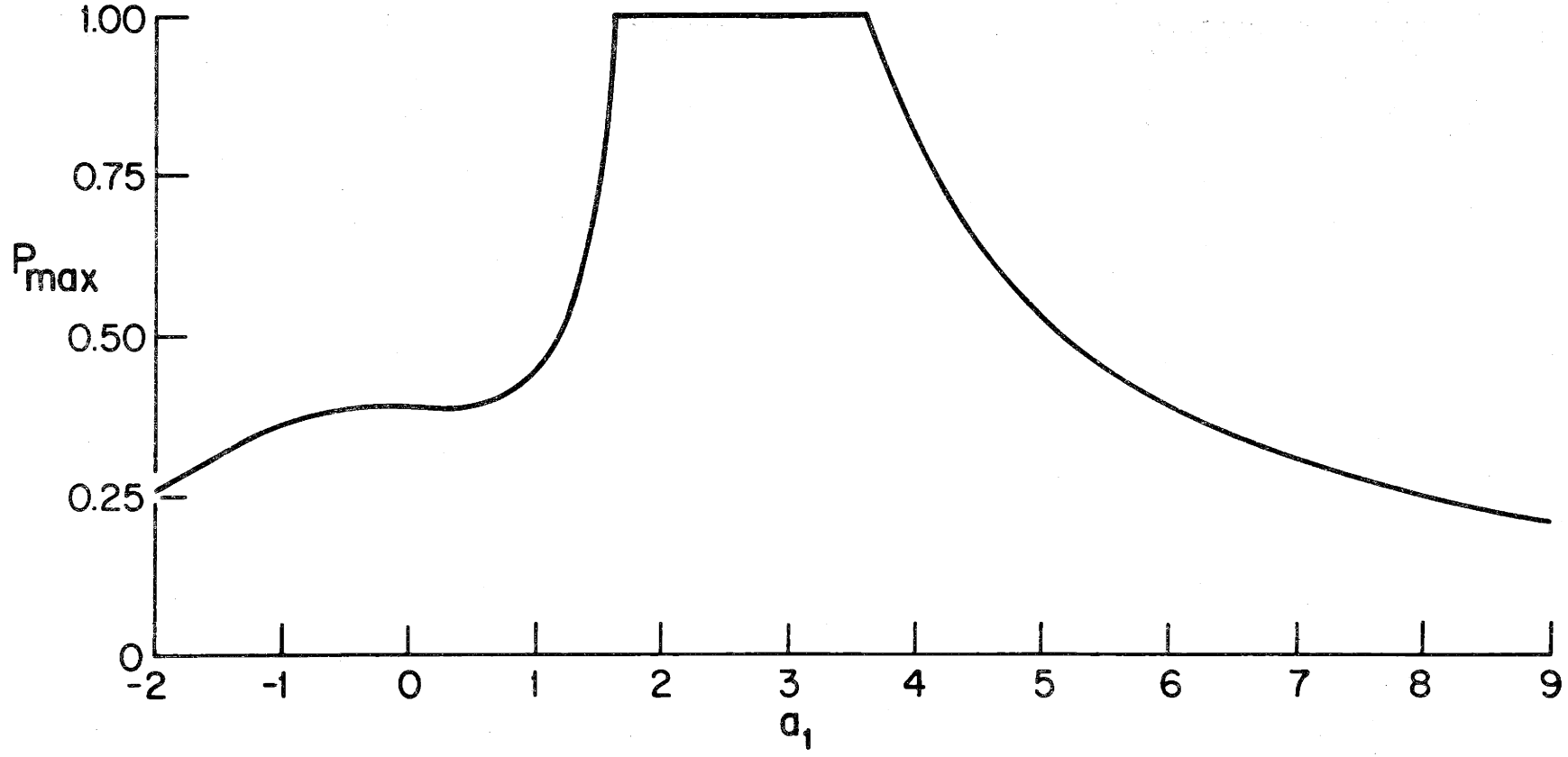

Figure 3.2 P_{max} vs. a_1 for a = 2.0

following intersection:

$$[P_{min}, 1] \cap [0, P_{max}]$$

As mentioned before, this interval $[P_{min}, P_{max}]$ is an important quantity in differentiating the cases used for examples.

Since the universally stable case is a type of "best case" MMAC system, the properties of this type of response were investigated. To demonstrate some of the properties, and to determine the accuracy of the RIDF, Case 1 was developed as a universally stable example. This case is defined in Table 3.1, along with the following cases.

Case 2 is a hyperbolic oscillation system, i.e., a system with no stable probability interval. This "worst case" MMAC system is precisely Greene's deterministic hyperbolically stable system in the stochastic version, i.e., with non-zero noise sources.

Cases 3 and 4 are two examples of Greene's mixed case MMAC system. They are used to demonstrate the effects of decreasing the stable probability interval, and the effect on the error in the RIDF approximation. Both of these cases have internal stable probability intervals.

Case 5 is another mixed case MMAC, but this system has an endpoint inclusive stable probability interval. This case is used to demonstrate some errors in the RIDF, and to demonstrate the accuracy of an approximation derived later.

In each of the five cases, sample means and sample covariances of the MMAC states are obtained from Monte Carlo simulations. The sample statistics are averaged over 100 runs. This number of runs led to an

Table 3.1: Stochastic Case Definition

Case	a	a_1	a_2	h	h_1	h_2	g	g_1	g_2	P_{min}	P_{max}
1	2.00	1.75	3.25	.809	.771	.914	1.618	1.349	2.971	0.00	1.00
2	2.00	0	0	.809	.500	.500	1.618	0	0	--	--
3	2.00	1.57	3.63	.809	.738	.930	1.618	1.159	3.378	0.05	0.95
4	2.00	1.57	7.909	.809	.738	.984	1.618	1.159	7.782	0.75	0.95
5	2.00	1.75	7.909	.809	.771	.984	1.618	1.349	7.782	0.75	1.00

acceptable scatter in the sample statistics, without the higher cost of averaging over a greater number of runs.

3.5 Stochastic Responses of MMAC Systems

In this section, insights into the stochastic response of the MMAC will be presented. These insights were obtained from Monte Carlo simulations, RIDF approximations, and analysis. Five different responses are used to demonstrate the properties of the stochastic MMAC system.

The MMAC system design uses nominal noise covariances, but in application the actual noise covariance may differ significantly from the nominal. This noise mismatch was found to have little effect on the nature of the response of the stochastic MMAC. The effects were limited to scaling the variances of the states, or in some cases, scaling the response of the variances in time. This time scaling effect is used in Case 4 to speed the response. All other simulations use the nominal noise covariances for the noise inputs.

The first case of interest is the universally stable MMAC, a globally asymptotically stable system. For a system of this type, the first two moments of the states should be finite, for bounded covariance inputs. This behavior is exhibited by both the Monte Carlo simulations and the RIDF prediction, Figure 3.3. It should also be noted that the RIDF accurately predicts the transients of these moments of the plant states.

Looking at this example, the response of the variance is quite similar to that of a stable linear system. This is not unexpected, since the MMAC system is linear for fixed P, and in this case, also stable for all P(k).

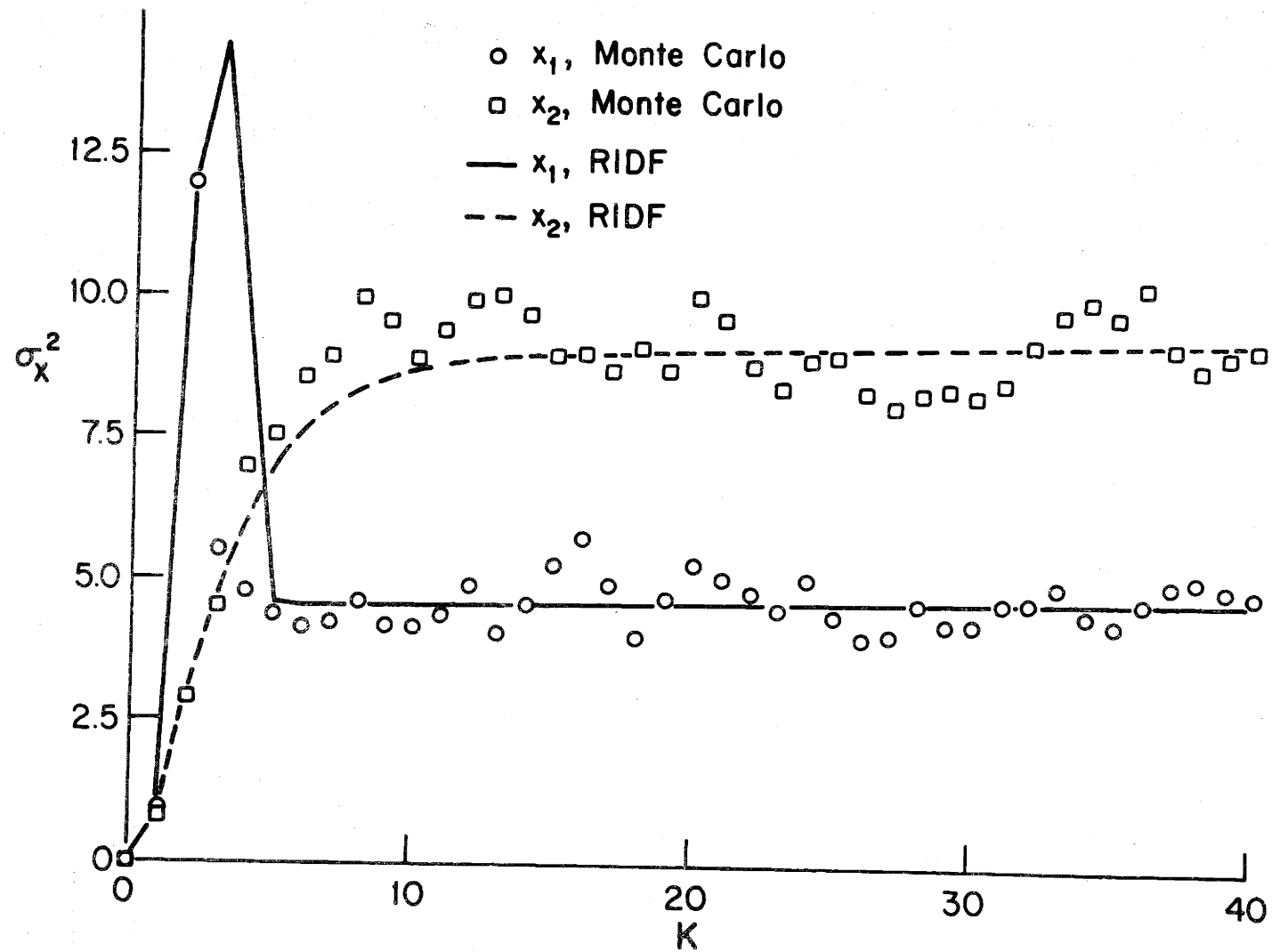

Figure 3.3 RIDF and Monte Carlo Plant State Variances (Case 1)

A look at the expected value for P(k) from the simulation explains the quasi-linear behavior. The expected value for P(k) approaches 1, therefore, this system is essentially linear after the initial time interval. In the following paragraph an approximation is derived for the probability density of P(k).

To gain further insight into the response of the MMAC system, an approximation for the density of P(k) is derived for the following case:

$$a_1 = a_2 \tag{3.58}$$

$$h_1 = h_2 \tag{3.59}$$

$$g_1 = g_2 \tag{3.60}$$

Moments of $\alpha(k)$ can be determined analytically. The equation for $\alpha(k)$, equation (3.7), is repeated here.

$$\alpha(k+1) = \alpha(k) + \underline{r}_1'(k+1)\underline{\theta}_1^{-1}\underline{r}_1(k+1) - \underline{r}_2'(k+1)\underline{\theta}_2^{-1}\underline{r}_2(k+1) \tag{3.7}$$

Letting

$$\Delta\alpha(k) = \underline{r}_1'(k+1)\underline{\theta}_1^{-1}\underline{r}_1(k+1) - \underline{r}_2'(k+1)\underline{\theta}_2^{-1}\underline{r}_2(k+1) \tag{3.61}$$

allows the following formulation for $\alpha(k+1)$:

$$\alpha(k+1) = \alpha(k) + \Delta\alpha(k) \tag{3.62}$$

In the case of a symmetric mismatched system,

$$E[\Delta\alpha(k)] = 0 \tag{3.63}$$

implying

$$E[\alpha(k)] = (0) \tag{3.64}$$

The second moment of $\alpha(k)$ can also be determined for this case:

$$E[\alpha^2(k+1)] = E[(\alpha(k) + \Delta\alpha(k))^2] \tag{3.65}$$

$$= E[E[\alpha(k)\Delta\alpha(k)|\alpha(k)]] + E[\alpha^2(k)] + E[(\Delta\alpha(k))^2] \tag{3.66}$$

$$= E[\alpha(k)E[\underline{r}_1'(k+1)\underline{\theta}_1^{-1}\underline{r}_1(k+1) - \underline{r}_2'(k+1)\underline{\theta}_2^{-1}\underline{r}_2(k+1)|\alpha(k)]]$$

$$+ E[\alpha^2(k)] + E[(\Delta\alpha(k))^2] \tag{3.67}$$

Due to the symmetric mismatch

$$E[\underline{r}_1'(k+1)\underline{\theta}_1^{-1}\underline{r}_1(k+1) - \underline{r}_2'(k+1)\underline{\theta}_2^{-1}\underline{r}_2(k+1)|\alpha(k)] = 0 \tag{3.68}$$

Therefore

$$E[\alpha(k)\Delta\alpha(k)] = 0 \tag{3.69}$$

Since

$$E[(\Delta\alpha(k))^2] > 0 \tag{3.70}$$

in all but the singular case where

$$\underline{\Sigma}_{r_1} - \underline{\Sigma}_{r_1 r_2}\underline{\Sigma}_{r_2}^{-1}\underline{\Sigma}_{r_2 r_1} = 0 \tag{3.71}$$

One example of this is where both models are the same, not a very interesting case. It was assumed, for the following analysis, that this singular condition did not hold, so that the mean square value of $\alpha(k)$ was greater than

zero. Then the second moment of $\alpha(k)$ is unbounded in this case, i.e.,

$$E[\alpha^2(k)] \xrightarrow[k \to \infty]{} \infty$$

If the residuals of the filters were Gaussian, the increment in α ($\Delta\alpha(k)$) would have a two sided chi square probability density, since $\Delta\alpha(k)$ would be the difference between two squared Gaussian random variables. With substantial measurement noise, the residuals were approximately Gaussian, so the probability density for $\alpha(k)$ (assumed to be two sided Chi Square) was approximated by the following.

$$f(\alpha) = \begin{cases} \frac{1}{\sigma_\alpha} e^{2(\alpha - m_\alpha)/\sigma_\alpha} & \alpha < m_\alpha \\ \frac{1}{\sigma_\alpha} e^{-2(\alpha - m_\alpha)/\sigma_\alpha} & \alpha > m \end{cases} \tag{3.72}$$

$$E[\alpha] = m_\alpha \tag{3.73}$$

$$E[(\alpha - m_\alpha)^2] = \sigma_\alpha^2 \tag{3.74}$$

The purpose of this assumed density was to determine an approximate density for P(k). The choice of this two-sided exponential was one of convenience. A comparison of using different two sided densities for $\alpha(k)$ showed little effect on the induced density of P(k), for large m_α and/or σ_α.

The induced density on P, assuming $f(\alpha)$ is the above (3.72) two sided exponential density, is the following.

$$f(P) = \begin{cases} \frac{2}{\sigma_\alpha} e^{-2m_\alpha/\sigma_\alpha} \left[\frac{1-P}{P} \right]^{\frac{4}{\sigma_\alpha}} \frac{1}{P(1-P)} & P > \frac{1}{1+e^{m_\alpha/2}} \\ \frac{2}{\sigma_\alpha} e^{2m_\alpha/\sigma_\alpha} \left[\frac{P}{1-P} \right]^{\frac{4}{\sigma_\alpha}} \frac{1}{P(1-P)} & P < \frac{1}{1+e^{m_\alpha/2}} \end{cases} \quad (3.75)$$

Figure 3.4 is a plot of this approximate density for P for various values of σ_α and $m_\alpha = 0$. This plot is indicative of the trend in f(P) as σ_α increases, as in the case of symmetric mismatch of the models. In this case, the limiting density of P approaches the following:

$$f(P) \simeq \tfrac{1}{2}\,\delta(P) + \tfrac{1}{2}\,\delta(P-1) \quad (3.76)$$

All of Greene's cases fit in the symmetric mismatch system class--in particular, the stable hyperbolic case which is examined now. In this case, the system is stable in the deterministic sense, but it is unstable for the stochastic case, as indicated in the simulators to be described later.

The proof of stochastic instability of the deterministic hyperbolically stable system has not been completed. The fact that the probability approaches the singular density, equation (3.76), for which the probability mass is concentrated at zero and one is not enough to prove instability of the system. Even though the system is unstable for these two points an alternation from P = 0 to P = 1 and back may stabilize the system in a manner similar to the deterministic response. In the stochastic case the expected trend in these peaks must be decreasing for the system to be stable. One way to show this would be a generalization of the deterministic work. To determine trends in the expected peak height, a conditional

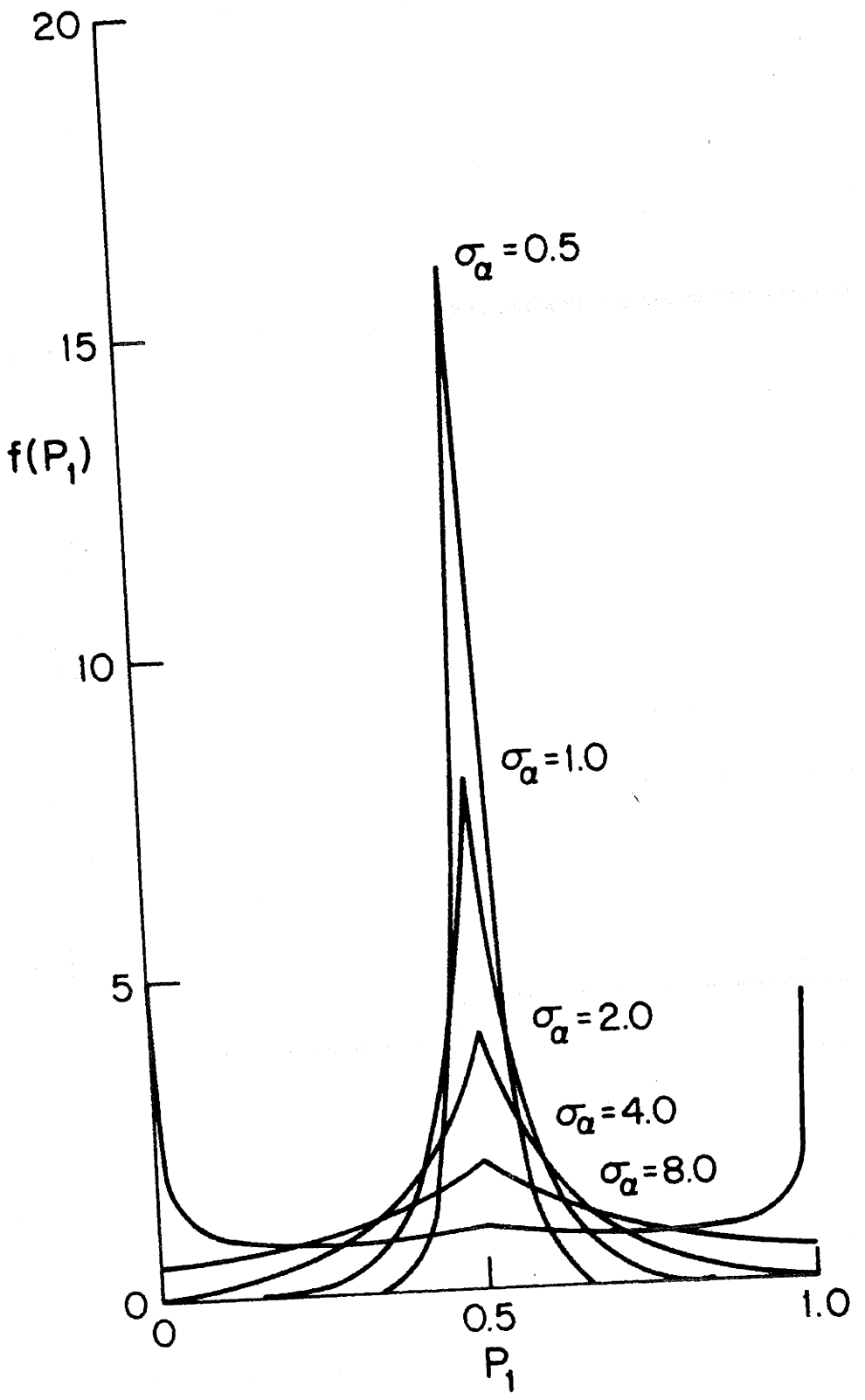

Figure 3.4 Approximate Probability Density for P

expected switch time could be computed. The conditioning would be on the present state of the MMAC system. The details of this approach are not trivial and have not been worked out.

Figure 3.5 is a plot of the variances of the plant states for this type of system (Case 2) for both the Monte Carlo simulation and RIDF approximation. The indication of instability is evident for both of these runs, but the quantitative prediction of the RIDF is seen to be in error.

In looking at the full covariance matrix for the MMAC states as predicted by the RIDF, it was found that the variance of $\alpha(k)$ approached a constant value, contrary to the behavior predicted in the analysis of $\Delta\alpha(k)$ and the Monte Carlo response. It is conjectured that inclusion of higher order moments of $\alpha(k)$ in the approximation, Geier [10], would improve the accuracy of the approximation. Verification of this conjecture was not pursued in this work.

The next two cases to be investigated are both internal stable probability interval cases. The first is quite close to the universally stable MMAC, in terms of the stable probability interval,

$$P_{stable} \in [.05, .95]$$

and the second is quite close to the hyperbolically stable system

$$P_{stable} \in [.75, .95]$$

With this large difference between the two systems' stable probability intervals, the responses are surprisingly similar.

Since the first case is almost universally stable the response might

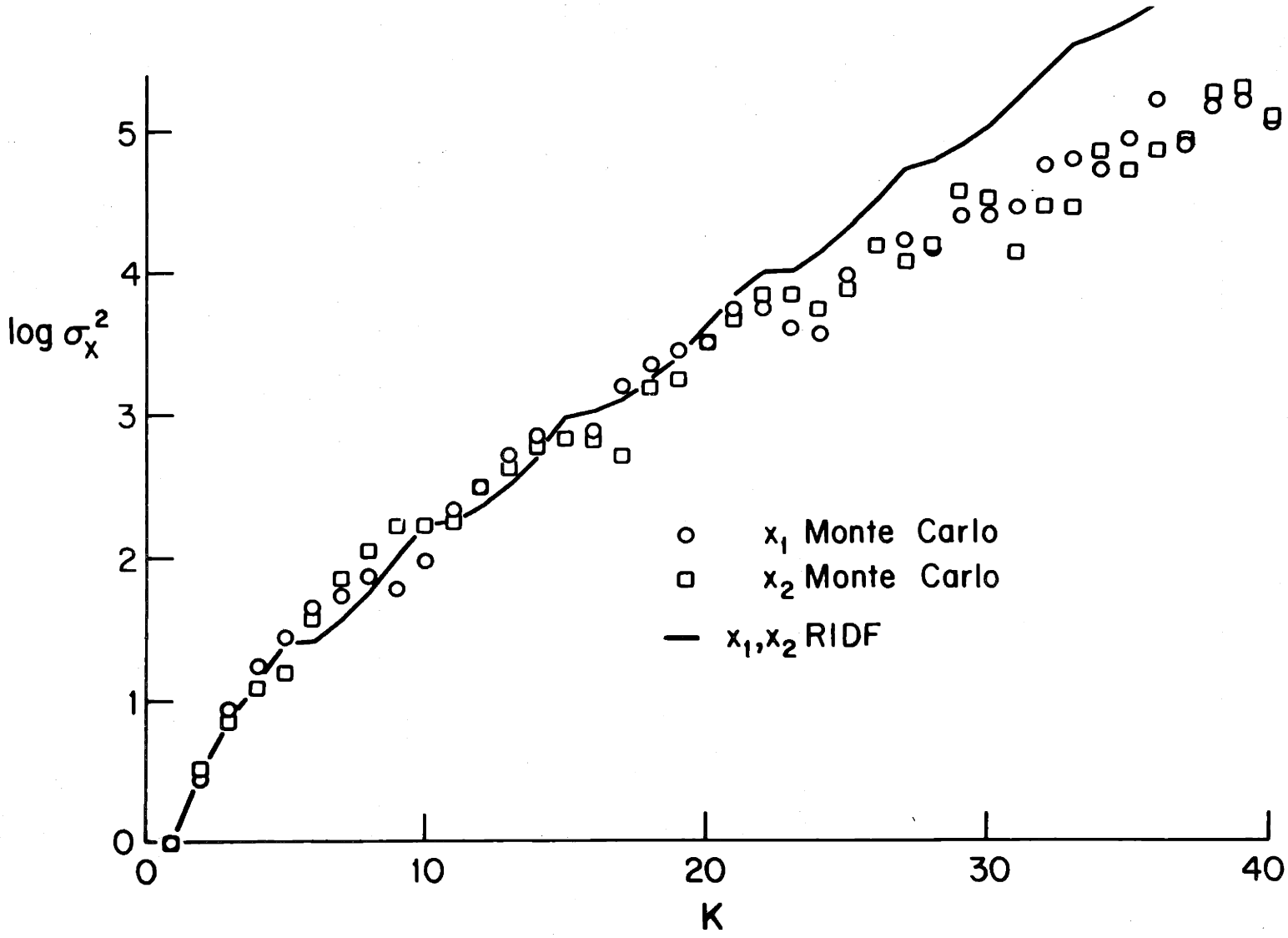

Figure 3.5 RIDF and Monte Carlo Plant State Variances (Case 2)

be expected to be similar to the universally stable system. This is not true, and this is demonstrated by looking at $P(\alpha(k))$. For the symmetric mismatch MMAC system, the mass of the probability density for P moves out of the stable interval for sufficiently large k, leading to an unstable response, i.e., growth of the variance of the plant states. Figure 3.6 is a plot of the variance of the plant states for both the Monte Carlo simulation and the RIDF prediction.

This effect is more pronounced in the second case with the smaller stable probability interval. A smaller $\sigma_\alpha(k)$ is sufficient in this case to have a large portion of the probability mass outside the stable interval. The smaller of the growth rates of the variances of the two plant states increases significantly as $\sigma_\alpha(k)$ becomes sufficiently large; consequently f(P) approaches a density with delta functions at zero and one. After this threshold is passed, the smooth growth rate changes to a more erratic growth.

This case is the only one where mismatched noise covariances were used. The actual covariances used for the noise inputs are

$$V = W = 100I \tag{3.77}$$

This mismatched noise covariance does not affect the type of response beyond the variance scaling and time scaling mentioned earlier. The threshold is attained in a shorter time with this larger covariance, Figure 3.7. Using nominal covariance noise sources would also result in the unstable behavior but it takes longer to develop (since the growth rate for $E[\alpha^2(k)]$ is smaller in the nominal case).

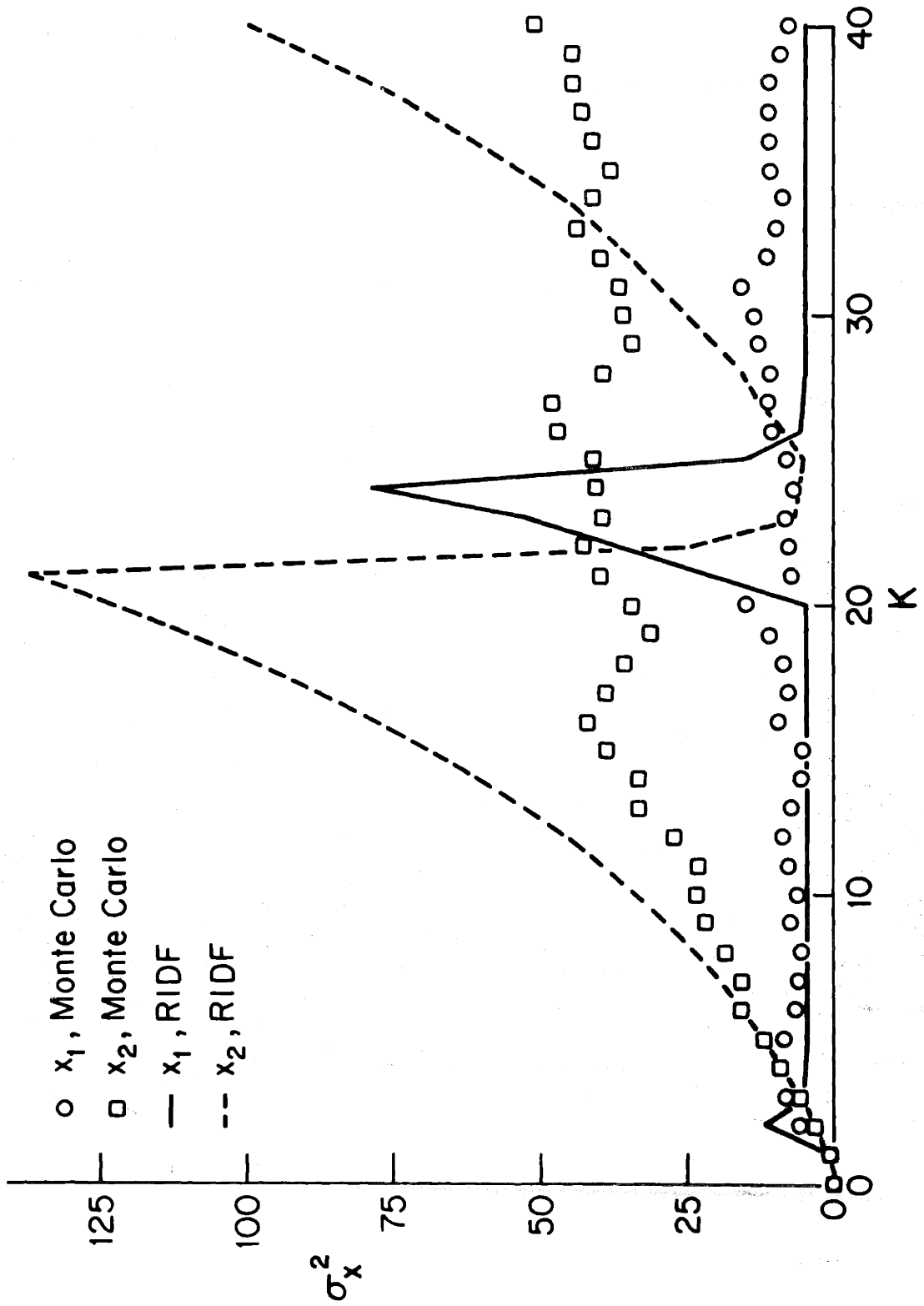

Figure 3.6 RIDF and Monte Carlo Plant State Variances (Case 3)

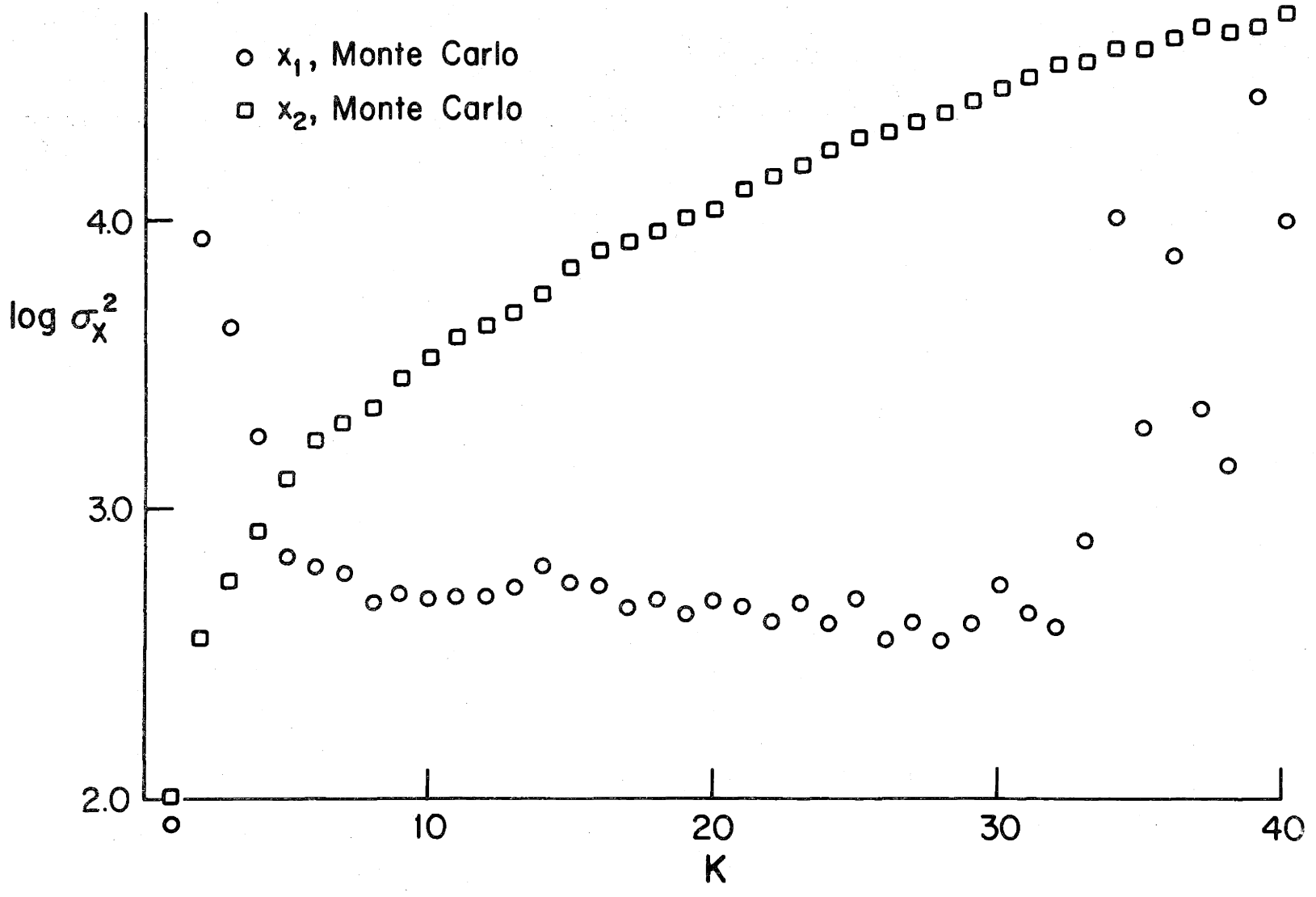

Figure 3.7 RIDF and Monte Carlo Plant State Variances (Case 4)

The last case presented is an endpoint inclusive stable probability interval MMAC system. This case is one of Greene's mixed case type MMAC systems. This MMAC system has a region of attraction behavior similar to the deterministic mixed cases. It is used to demonstrate the error in the RIDF and to demonstrate the accuracy of another approximation derived next.

This case does not have the symmetric mismatch mentioned earlier, so

$$E[\Delta\alpha(k)] \neq 0 \tag{3.78}$$

With this drift in $E[\alpha(k)]$, the probability density for $P(k)$ accumulates at $P = 1$. To get a handle on the rate of drift of $E[\alpha(k)]$, $\Delta\alpha(k)$ will be investigated in more detail.

$$\Delta\alpha(k) = \underline{r}_1'(k+1)\underline{\theta}_1^{-1}\underline{r}_1(k+1) - \underline{r}_2'(k+1)\underline{\theta}_2^{-1}\underline{r}_2(k+1) \tag{3.61}$$

Replacing $\underline{r}_1(k+1)$ and $\underline{r}_2(k+1)$ in equation (3.61) using equations (3.13) - (3.14) results in the following (the time dependence k, k+1 having been dropped):

$$\begin{aligned} E[\Delta\alpha] = E[&(\underline{A}\underline{x}-\underline{A}\hat{\underline{x}}_1+\underline{v}+\underline{w})'\underline{\theta}_1^{-1}(\underline{A}\underline{x}-\underline{A}_1\hat{\underline{x}}_1+\underline{v}+\underline{w}) - (\underline{A}\underline{x}-\underline{A}_2\hat{\underline{x}}_2+\underline{v}+\underline{w})'\underline{\theta}_2^{-1} \\ &\times (\underline{A}\underline{x}-\underline{A}_2\hat{\underline{x}}_2+\underline{v}+\underline{w})] \end{aligned} \tag{3.79}$$

Assuming the second moments of $\underline{x}$, $\hat{\underline{x}}_1$ and $\hat{\underline{x}}_2$ are approximately equal

$$\begin{aligned} E[\Delta\alpha] \simeq \mathrm{tr}[&(\underline{\theta}_1^{-1}[\underline{A}\underline{A}'-2\underline{A}\underline{A}_1'+\underline{A}_1\underline{A}_1'] - \underline{\theta}_2^{-1}[\underline{A}\underline{A}'-2\underline{A}\underline{A}_2'+\underline{A}_2\underline{A}_2'])E[\underline{x}\underline{x}'] \\ &+ (\underline{\theta}_1^{-1}-\underline{\theta}_2^{-1})(\underline{V}+\underline{W})] \end{aligned} \tag{3.80}$$

It should be noted that the assumption on the second moments of $\underline{x}$, $\hat{\underline{x}}_1$ and $\hat{\underline{x}}_2$ is crucial to this approximate analysis. Although it holds for the example case, in general it may be unfounded. So with these assumptions, an approximation to the expected drift in $\alpha(k)$ as a function of the input noise covariance and second moment of the plant states can be derived.

For Case 5, the approximation for $E[\Delta\alpha]$ is the following.

$$E[\Delta\alpha] \simeq tr\left[\begin{bmatrix}-17.6 & 0\\ 0 & .03\end{bmatrix} E[\underline{x}\underline{x}'] + \begin{bmatrix}.049 & 0\\ 0 & .012\end{bmatrix} (\underline{V}+\underline{W})\right] \tag{3.81}$$

if $E[\underline{x}\underline{x}']$ dominates $(\underline{V}+\underline{W})$ then

$$E[\Delta\alpha] \simeq \begin{bmatrix}-17.6 & 0\\ 0 & .03\end{bmatrix} E[\underline{x}\underline{x}'] \tag{3.82}$$

Due to the structure of the MMAC system, the input noise filters through both plant states, i.e., the V_1 input will affect the plant state x_2 in the diagonal case investigated in this thesis. This leads to the situation where

$$E[x_1^2] \simeq E[x_2^2] \tag{3.83}$$

for the two model case. For Case 5, the above assumptions were found to be reasonable. Consequently, the prediction of

$$E[\alpha(k)] \xrightarrow[k\to\infty]{} -\infty$$

was accurate.

With $E[\alpha(k)] \rightarrow -\infty$, the mass of the probability density for P(k) will accumulate at one and zero, i.e., f(P) will approach the following:

$$f(P) \Rightarrow q\delta(P) + (1-q)\delta(1-P)$$

The weight, q, will depend on the relative rates of growth of m_α and σ_α.

With P(k) approximately one, the system is stable, so only the noise inputs will drive P(k) away from one. If the sequence of $\Delta\alpha(k)$ make $\alpha(k)$ large, positively, the system will be unstable for the corresponding P(k) (P(k) = 0). So the states will grow, particularly state x_1. This increase in the states will drive $\alpha(k)$ negative, where the system is stable. This behavior has been observed in several individual simulation runs which were run for a longer period than the Monte Carlo simulations described earlier.

Figure 3.8 is a plot of the Monte Carlo variances and the RIDF variances. As is seen in the time history of the variances, the RIDF is grossly in error for this case. Again, inclusion of higher moments in the computation of $\alpha(k)$ is thought to improve this error, Geier [10].

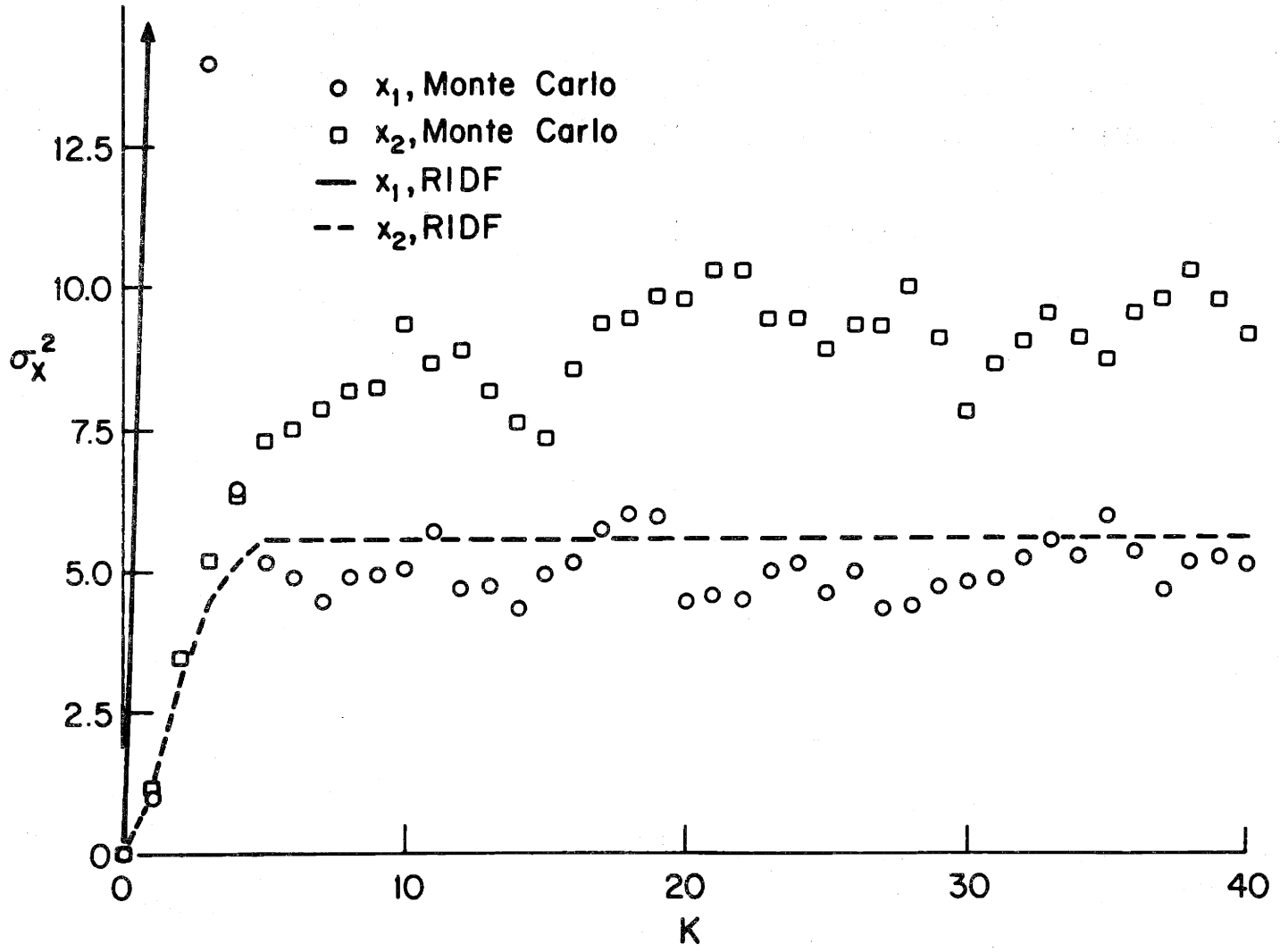

Figure 3.8 RIDF and Monte Carlo Plant State Variances (Case 5)

CHAPTER 4

CONCLUSIONS

In the prior two chapters, results of research into the properties of the MMAC algorithm have been presented. Techniques for analysis and insights into the behavior of the MMAC algorithm comprise the results of this work. In this chapter, the major results of this work will be reviewed, along with discussion concerning their significance, interrelation, and suggestions for future work.

4.1 Deterministic MMAC Conclusions

In the deterministic work, three approximations were investigated, each for a different class of MMAC systems. In the case of the full memory MMAC systems, Greene's approximation was found to be in error when implemented. The norm $||\underline{A}||^2$ was too conservative when used in the approximation, the rates of growth of the states were predicted incorrectly. In this approximation, $||\underline{A}||^2$ was not used as a bound, but it was used to reflect the rate of growth of the states. It was found that the quasi-norm $||\underline{A}||_*^2$ more accurately approximated the rate of growth of the states. In future use of this approximation, replacement of $||\underline{A}||^2$ by $||\underline{A}||_*^2$ will result in a more accurate approximation in most cases. In analyzing the accuracy of the approximations for deterministic MMAC systems, this replacement has been made.

For the cases that have been considered, the accuracy of the modified

approximation is quite good. The stability indications are accurate, as are the predictions of the rates of growth or decay of the magnitudes of the peaks. The trends in the length of the interval between switches in the probability are also accurately predicted.

Although the accuracy was good for the simple cases examined, it might be worse for higher order stiff systems. For the more complex systems, this modified approximation may also be conservative. The predicted rates of decay and growth may be such that a prediction of instability may be made for a system that is stable. This is the same type of error that was found for the approximation using $\|\underline{A}\|^2$.

The second approximation was one derived for the response of the limited memory MMAC system. This approximation was derived in a manner similar to Greene's, and exhibited similar accuracy for unstable and neutrally stable hyperbolic MMAC systems. For these two cases, the responses were hyperbolic oscillations, but at a higher frequency. The approximation correctly predicted the stability (unstable, and neutrally stable) of the systems. Although the prediction of high frequency was qualitatively correct, the actual switching frequency exhibited in the simulations was somewhat slower than the predicted frequency.

For the hyperbolically stable MMAC system, the prediction of the approximation for this limited memory case was in error. The approximation predicted an asymptotically stable response, when the simulated response was neutrally stable. Insight into the response of the limited memory MMAC was gained in determining the cause for this erroneous prediction.

The magnitudes of the states decrease with time for the full memory hyperbolically stable MMAC system. With large initial conditions, this is also the case for the limited MMAC, during the initial time interval. In the limited memory case as the magnitudes of the states decrease to zero, the probability (P(k)) goes to ½. If the linear system for P(k) fixed at ½ is unstable, the magnitude states will grow, driving P(k) away from ½. Consequently, the system will have a limit cycle response. This is one explanation for response observed in the simulations. In addition the derivation of the approximation for the limited memory MMAC system assumed that P = 0 or P = 1. In hyperbolically stable system limited memory response outlined above, it is observed that P takes on values around ½, violating the assumption used in the derivation. With this assumption, the possibility of a limit cycle response described above is ignored, so the approximation will be in error for this case.

As a check on the results presented for this last case, a modified control was used for the MMAC system. This maximum likelihood control is equivalent to ensuring P = 0 or P = 1. This modification does not change the approximate analysis for the limited memory MMAC; the maximum likelihood control guarantees the switch-like behavior of the probabilities assumed in the approximate analysis. In contrast to the limit cycle behavior exhibited earlier, this maximum likelihood control MMAC system had an asymptotically stable response. For this case, the predicted rate of decay of the states was accurate. Again the qualitative prediction of high frequency switching in the probability was correct, although the actual rate was somewhat slower than predicted.

This analysis of the limited memory MMAC system has brought to light an interesting effect of modifying the control used in the algorithm. If one of the models matches the actual plant dynamics, the full memory MMAC will lock on to that model. If none of the models match, the limited memory may do better, because the full memory MMAC may lose its adapability in locking into one model. In limiting the memory, the smoothing of the probabilities in the full memory MMAC is sacrificed for adaptability. Using the maximum likelihood control in the limited memory MMAC improves the stability of the overall system in some cases. How well this stabilizing property of the maximum likelihood control MMAC applies in more complex systems needs to be investigated.

The last approximation derived, was for the case where constant biases in the control inputs were allowed. The approximation for this class of problems was found to have good accuracy in predicting the switch times and the magnitudes of the peaks. In the case where the biases are zero this approximation reduces to Greene's approximation. The effects of the mismatched models was accentuated by the biased inputs. In the approximation, the bias effects dominated some effects which led to the errors in the approximate analysis in the non-biased case.

The response of the hyperbolically stable MMAC for this case of biased inputs was found to be unstable. Hyperbolic stability depends on a tenuous balance of alternately stabilizing and destabilizing the states, which the biases overwhelm. Consequently, the magnitudes of the peaks grow with time. This instability indicates a need for a stronger stability condition for this case. An equation for determining the stability

was derived, but no simple condition, similar to Greene's for the unbiased case, has been obtained from this equation.

4.2 Stochastic MMAC Conclusions

In the study of the stochastic MMAC systems, a two-fold approach was used to gain insights into the stochastic response. A RIDF approximation was derived, and checked against cases representative of the various responses of the class of MMAC systems studied. In checking this approximation, further insights into the characteristic responses of the MMAC were gained. In parallel with the RIDF work, some other, more exact analysis led to some interesting results and insights.

In checking the RIDF approximation, five cases were used, each representing different types of deterministic system behavior. In the cases where the RIDF predicted a stable response for the first two moments of the MMAC states, the predicted values were very accurate when compared to Monte Carlo simulation results. Only in one of the five cases was there a discrepancy between the qualitative prediction of the RIDF and the Monte Carlo simulation.

In checking the response of the first two moments of the log likelihood ratio, $\alpha(k)$, it was conjectured that the RIDF does not account for the effects of higher order moments in the distribution of $\alpha(k)$. These effects can be included using a method similar to the modified CADET investigation by Geier [10]. Future work in this area might lead to an improvement in the qualitative predictions of the RIDF.

As mentioned above, the RIDF approximation was in error qualitatively

for one case. For this case the RIDF predicted the system was unstable, when the corresponding simulations indicated the system was stable. Investigating causes for this erroneous instability prediction led to significant insights into the stochastic MMAC system. For a specific class of MMAC systems, those where the expected value of $\alpha(k)$ is constant, it was determined analytically that the variance of $\alpha(k)$ grew without bound, implying that the corresponding density of $P(k)$ is singular at $P(k) = 0$ and $P(k) = 1$. Approximate analysis of the density of $\alpha(k)$, where the mean value is not constant, also leads to this conclusion. The relative weights of the delta functions at zero and one, for the limiting density of $P(k)$, are determined by the relative rates of growth of the mean and variance of $\alpha(k)$. The unbounded growth of the variance of $\alpha(k)$ is not predicted by the RIDF. It is conjectured that implementing Geier's [10] modified CADET, mentioned earlier, in the RIDF to include higher order moments of $\alpha(k)$ will improve the accuracy of the predictions of the variance of $\alpha(k)$.

The stable probability interval is an important factor in determining the stability of a stochastic MMAC system. Since the density of $P(k)$ approaches a singular density for a large class of MMAC systems, whether the stable probability interval includes the singular points of the limiting density or not clearly plays a crucial role in determining the stability of the system.

The endpoint inclusive stable probability interval MMAC system is the only case where the RIDF prediction of instability was in error. The prediction of a finite variance for $\alpha(k)$ disagrees with the analysis

indicating the variance should be unbounded. An approximation to the drift in the expected value of $\alpha(k)$ indicates that the expected value of $\alpha(k)$ is driven toward the stable end point. Consequently, the weighting of the delta function at the stable end point will be much greater than the weighting at the unstable end point, in the limiting density of P(k). The relative length of time that P(k) stays at the stable end point versus the unstable end point will determine the stability of the system. The relative length of time spent at each end point is dependent upon the time correlation of P(k), which, in general, has not been derived. Independent of correlation of P(k), the much lower probability associated with the unstable end point leads to the conjecture of stability for this end point inclusive MMAC system.

It is conjectured that the internal stable probability interval MMAC systems are unstable. In the deterministic equivalent of these stochastic systems, Greene's mixed case MMAC, P(k) will converge to a value within the stable interval. In the stochastic case, P(k) is driven outside the stable interval, as is seen in the limiting density of P(k). The singular points of the limiting density lie outside the stable interval, implying that the system should be unstable.

One possible mechanism for stability for systems with internal stability intervals is stochastic hyperbolic stability, a stochastic analog of Greene's deterministic hyperbolic stability. Instead of the precise switch-like behavior of the probabliity, observed in the deterministic hyperbolic system, P(k) would have a stochastic switch-like behavior. The stability of this system would depend on the time correlation of P(k).

Stochastic hyperbolic stability may also be possible for Greene's hyperbolically stable case, but it has not been observed in simulations of hyperbolic or internal stability interval MMAC systems.

For the deterministic hyperbolically stable MMAC system, introduction of biased inputs (set point MMAC) was sufficient to destabilize the system. It is possible that the stochastic end point inclusive MMAC system may also be destabilized by biased controls. The biases may drive $\alpha(k)$ away from the stable end point, i.e., the biases may overcome the drift in $\alpha(k)$ toward the stable endpoint. It is possible that this may lead to an unstable system, but this effect has not been investigated in this work.

As mentioned before, for a large class of MMAC systems, the probability density for P(k) degenerates to delta functions at zero and one. As P(k) approaches zero or one, the MMAC loses its adaptability. In practice, the adaptability of the MMAC is one of the major reasons for using it; loss of this ability to reflect changing operating conditions is not desirable. To eliminate this degenerate probability density for P(k) (concentrated at zero or one), one of two methods can be used. The range on $\alpha(k)$ can be limited or $\alpha(k)$ can be age weighted, Greene [6]. For the two modifications, the mass of the probability density for P(k) is spread more uniformly between zero and one. With limit on $\alpha(k)$, the density of P(k) will have delta functions at the values which correspond to limits on $\alpha(k)$. The age weight modification will lead to concentrations of the density of P(k) at the end points (no delta functions). The effects of these modifications are similar, so discussion will be restricted to the limiting $\alpha(k)$ modification.

The limiting $\alpha(k)$ modification can either stabilize an unstable system or destabilize a stable system. If the limits on $\alpha(k)$ are chosen such that the corresponding limits on P(k) are within the stable probability interval, the system will be stabilized[1], Figure 4.1a. Also, if the limits on $\alpha(k)$ are such that the interval between the limits on P(k) does not intersect the stable probability interval, the system will be destabilized, Figure 4.1b. For the third possibility, where the interval formed by the limits on P(k) intersects the stable interval the stability depends on the time correlation of P(k), Figure 4.1c, as discussed previously.

4.3 Additional Directions for Future Work

As mentioned in the introduction, the work toward understanding the response of the MMAC system has been motivated by the F-8C application. Greene's work and the work presented in this thesis represent two steps toward gaining a full understanding of the MMAC system. In the last section a few directions for future work have been outlined. In this section, more directions for future work are described.

Most of the work done towards understanding the MMAC has assumed diagonal A matrices with identity B and C matrices. This class of systems, although sufficient to demonstrate some of the basic properties of the MMAC systems, is restrictive. The effects of relaxing these assumptions needs to be investigated. This would give more practical importance to the results obtained thus far.

[1]Since the computation of stable probability interval requires knowledge of the actual system dynamics, this is not a design procedure.

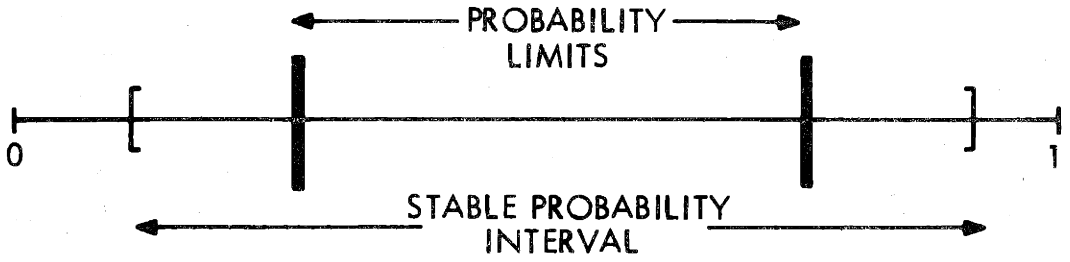

(a)

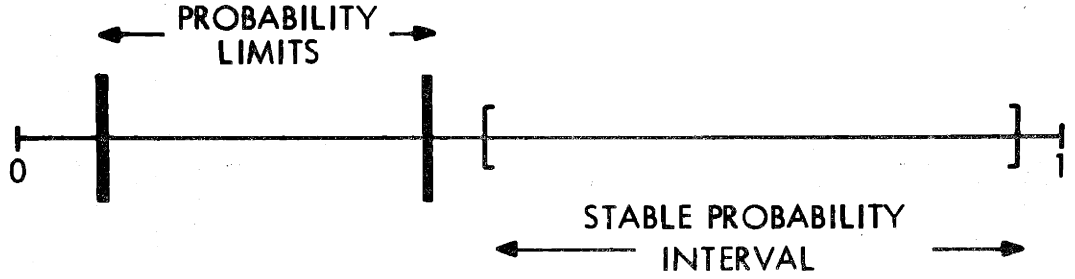

(b)

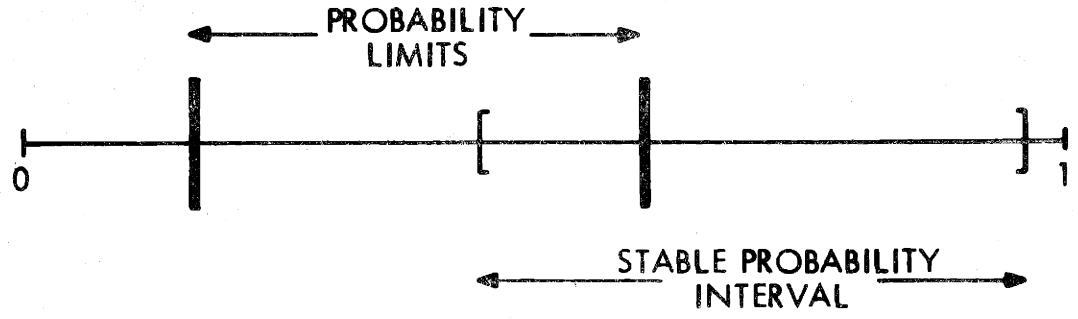

(c)

Figure 4.1 Probability Limits and Stable Probability Intervals

Thus far most of the research into the behavior of the MMAC system has been limited to the two model case. Extending the results of the two model MMAC to the N-model case would represent a quantum jump in the research of MMAC systems.

Another extension would be to investigate the MMAC properties for systems with nonlinear plants. The models for this application might be linearizations about equilibrium, as in the lateral dynamics of the F-8C [5], or linearizations about some other point in the state space, as in the longitudinal dynamics of the F-8C. This second linearization will have models with biases, resulting in biased control inputs. So the results of set point control MMAC will be useful in this application.

The work outlined here would provide the basis for a complete design methodology for the MMAC algorithm. Questions remain unanswered as to how close the models must be to the plant, or the number of models needed to stabilize a nonlinear plant through its full operating regime. The results of research for this thesis along with the work proposed in this chapter would provide the basis for determining how useful the MMAC algorithm is in specific applications and how to use it.

REFERENCES

1. Athans, M. and P. L. Falb, Optimal Control, New York: McGraw-Hill, 1966.

2. Pontryagin, L. S., V. Boltyanskii, R. Gamkrelidze and E. Mishchenko, The Mathematical Theory of Optimal Processes, New York: Interscience Publishers, Inc., 1962.

3. Bryson, A. E. and Y. C. Ho, Applied Optimal Control, Washington, D.C.: Hemisphere Publishing Corp., 1975.

4. Willner, D., Observation and Control of Partially Unknown Systems, MIT, PhD thesis, May 1973.

5. Athans, M., D. Castanon, K. P. Dunn, C. S. Greene, W. H. Lee, N. R. Sandell Jr. and A. S. Willsky, "The Stochastic Control of the F-8C Aircraft Using a Multiple Model Adaptive Control Method - Part 1," IEEE Trans. on Automatic Control, Vol. AC-22, pp. 768-780, 1977.

6. Greene, C. S., An Analysis of the Multiple Model Adaptive Control Algorithm, MIT, PhD thesis, August 1978.

7. Jazwinski, A. H., Stochastic Processes and Filtering Theory, New York: Academic Press, 1970.

8. Gelb, A. and W. E. VanderVelde, Multiple-Input Description Functions and Nonlinear System Design, New York: McGraw-Hill, 1968.

9. Chen, T. C., Introduction to Linear System Theory, New York: Holt, Rinehart and Winston, Inc., 1970.

10. Geier, G. J., Approximate Direct Statistical Analysis of Nonlinear Systems, MIT, M.S. thesis, 1973.